

Analisi della tessitura nei materiali tramite diffrazione neutronica

Luca Lutterotti

Università degli Studi di Trento

Dipartimento di Ingegneria dei Materiali e delle Tecnologie Industriali

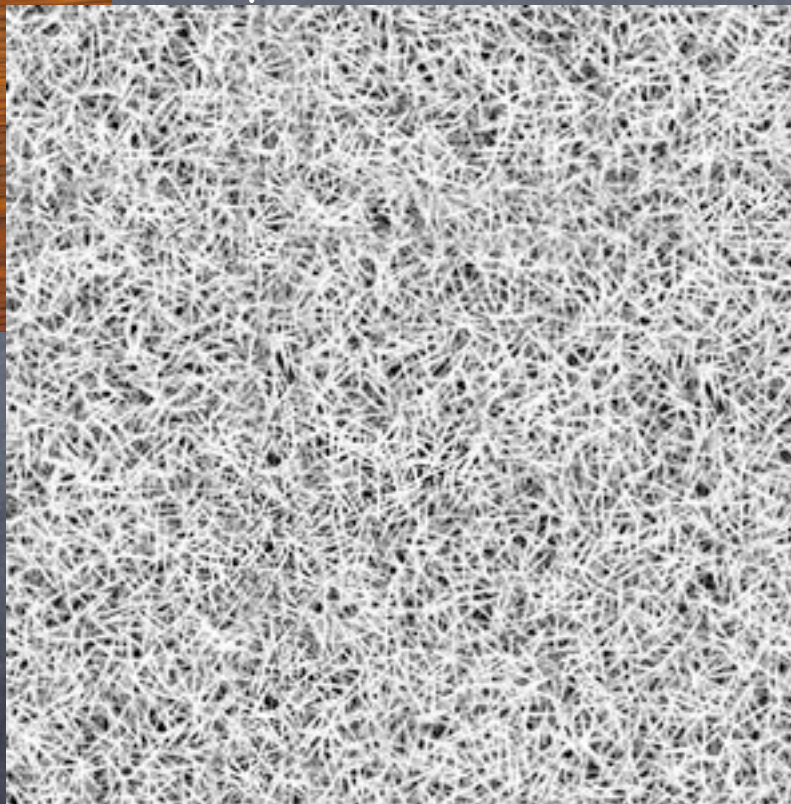
Outline

- ⦿ Introduction
 - ⦿ Texture analysis and neutron
 - ⦿ Rietveld Texture Analysis
 - ⦿ The method and algorithms
- ⦿ Analysis examples
 - ⦿ Texture and Earth Science
 - ⦿ Textured ceramic matrix composites
 - ⦿ The copper age axes
 - ⦿ Texture and memory effects in metals
- ⦿ Conclusions and future work

Texture and anisotropy



Wood: high resistance
parallel to fiber



Random textile

Textile: generally
bidirectional



Crystallographic texture



Random lunar rock (Apollo 12)



Porfritic texture



Intergrowths



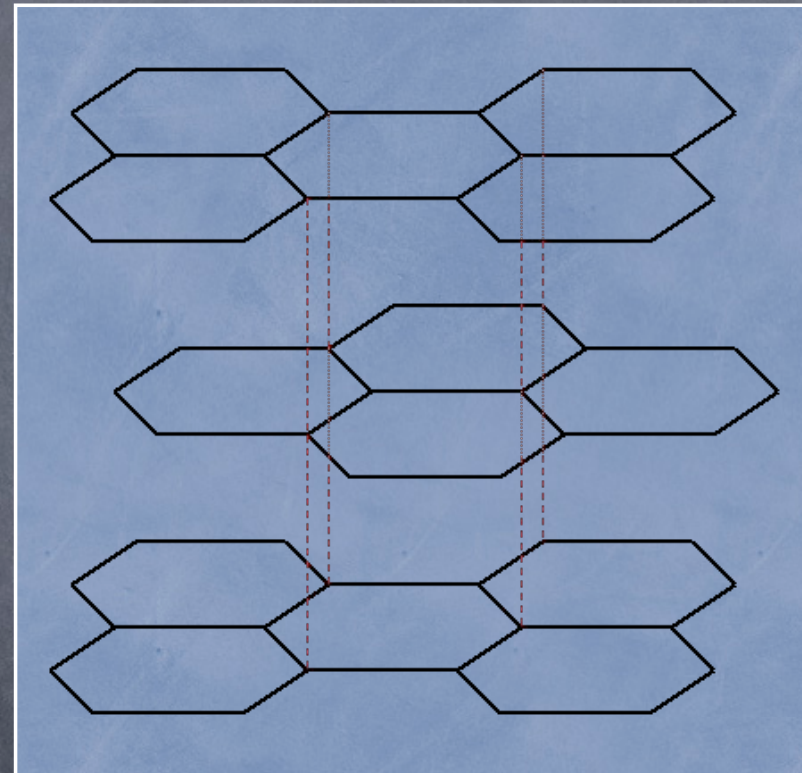
Platelet grains with ab
orientation for ceramic
superconductor
 $\text{Bi}_2\text{Sr}_2\text{CaCu}_2\text{O}_x$

Different color = different crystallographic orientation

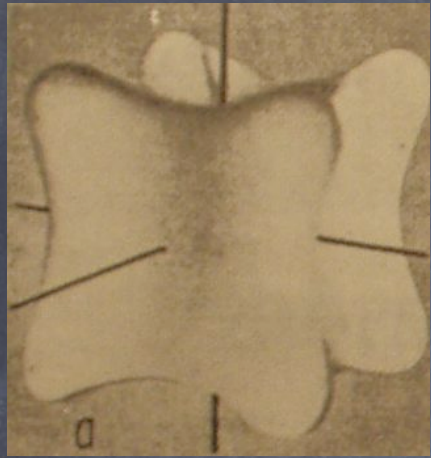
Single crystal anisotropy: graphite

Anisotropic properties:

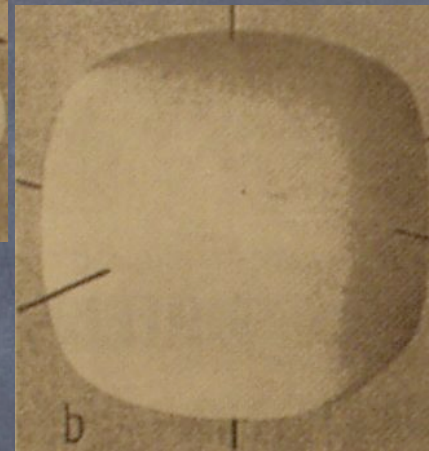
- ⦿ Electrical properties
- ⦿ Mechanical properties: elastic modulus, fracture, strains....
- ⦿ Thermal expansion
- ⦿ Thermal conductivity
- ⦿ Magnetic properties
- ⦿



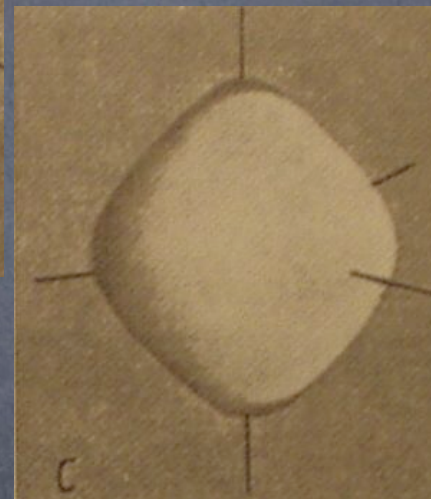
Elastic tensor anisotropy



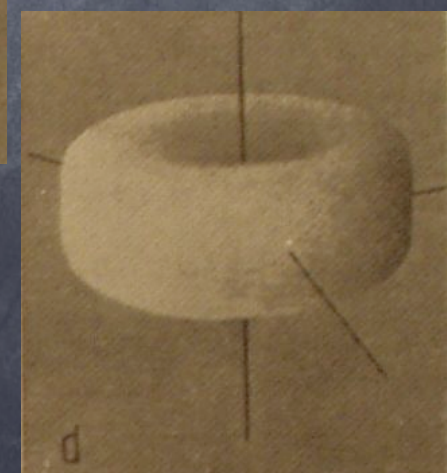
Au



Al



Mg



Zn

Anisotropic macroscopic properties



+



=



Anisotropic macroscopic properties

Definition

ODF: Orientation Distribution Function, $f(g)$

$$f(g)\Delta g = \frac{\Delta V(g)}{V}$$

Macroscopic properties:
e.g. elastic tensor, C

$$\overline{\underline{C}^{-1}}^a = \int_G \underline{C}^{-1}(g) f(g) dg$$

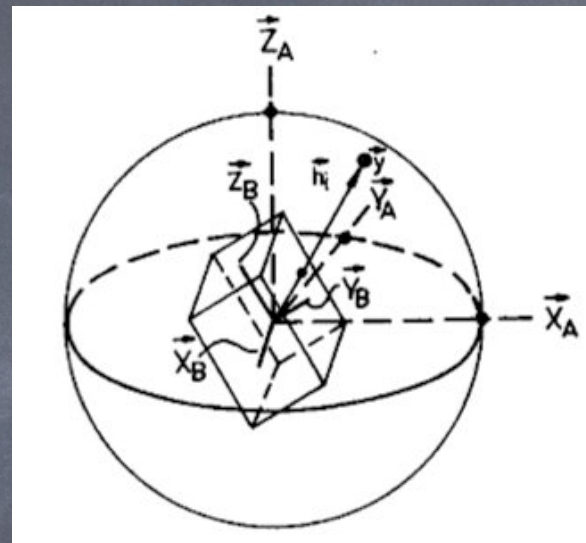
Reuss average

Pole figure

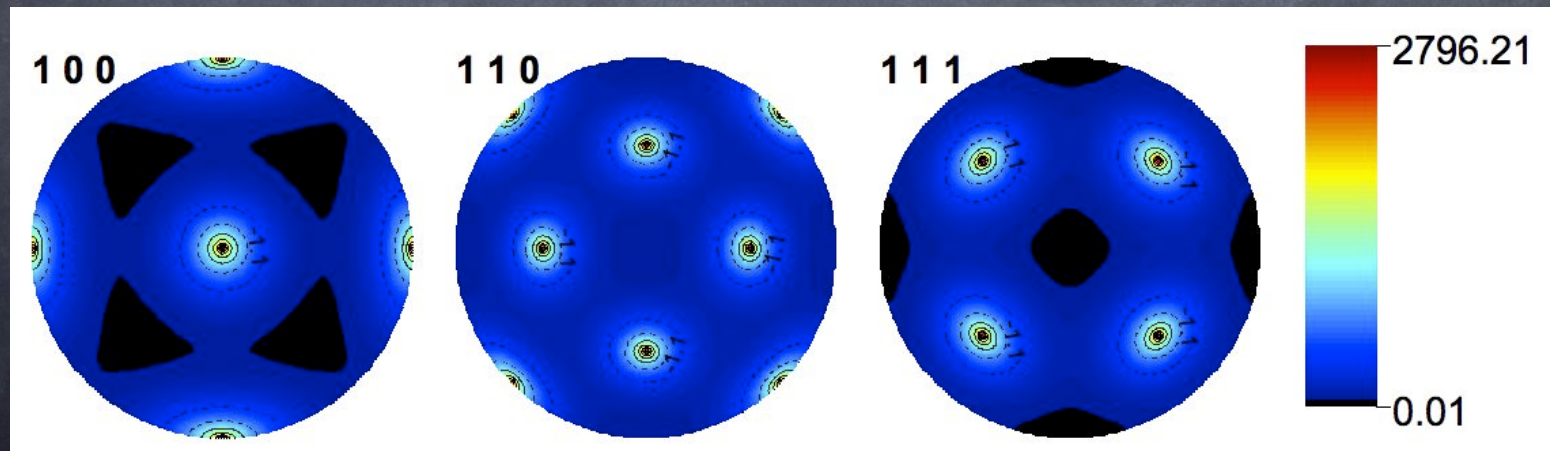
$$P_k(\chi, \phi) = \int_{\varphi} f(g, \varphi) d\varphi$$

Pole figure representation

A pole figure is a projection in 2D of the ODF for a specific (hkl) plane

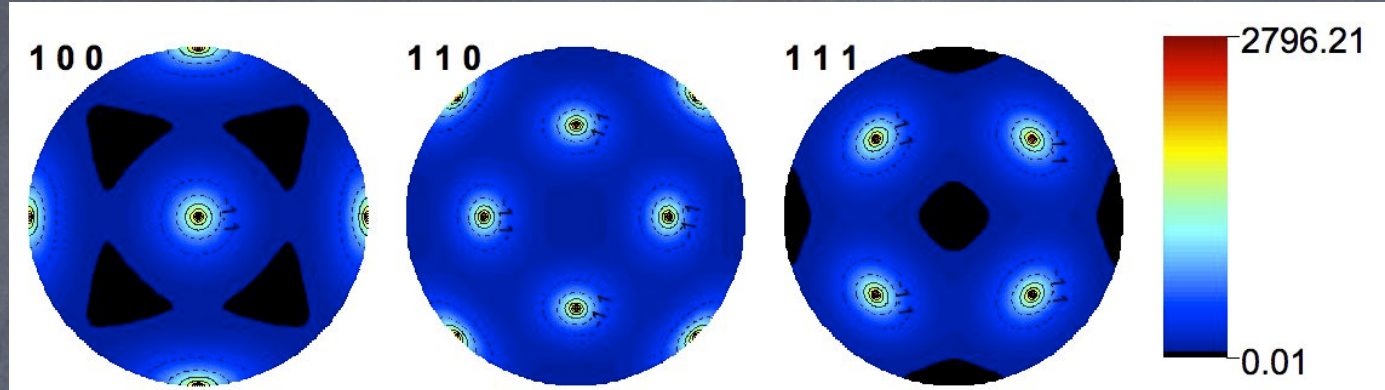


Cubic single crystal

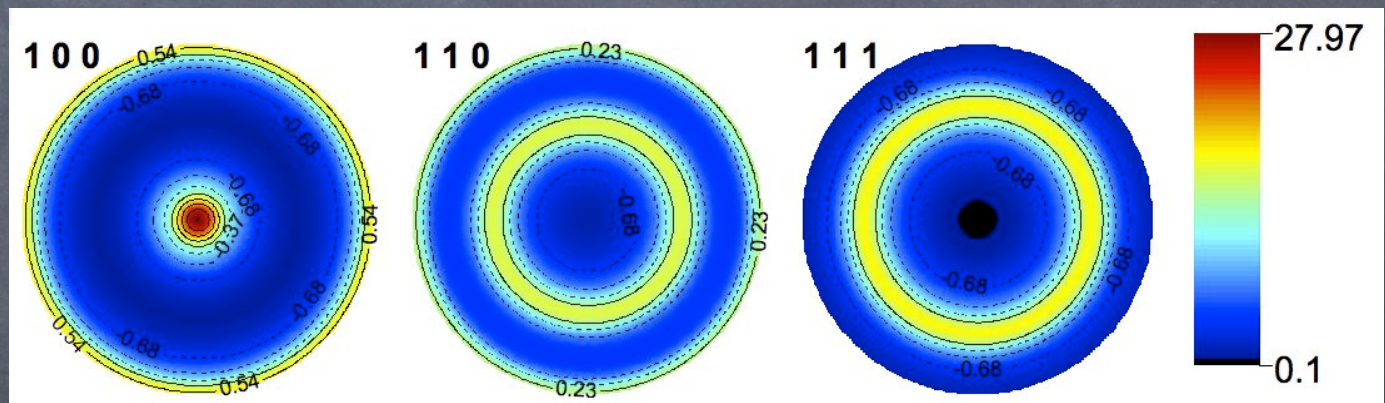


PF examples: From single crystal to laminate

Single crystal

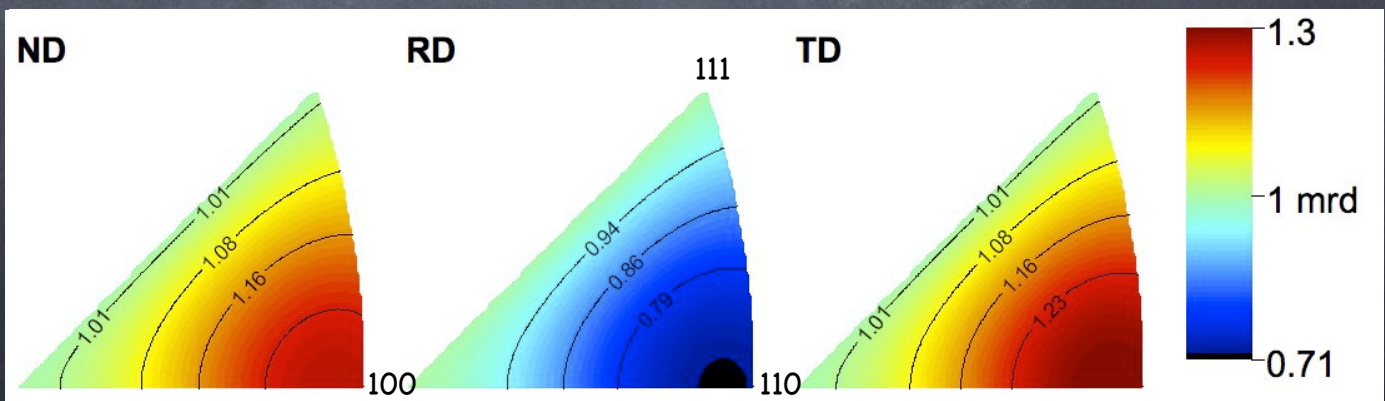


Fiber texture



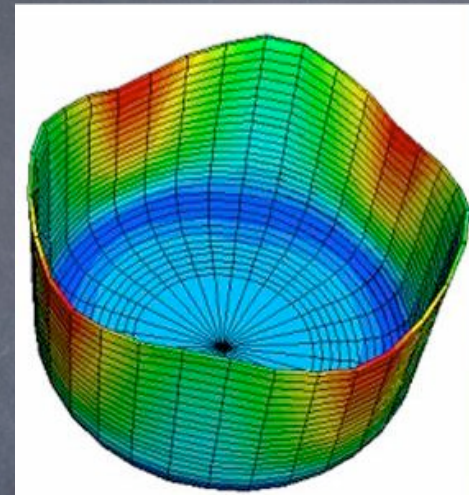
Laminate

Inverse pole
figures



Texture examples

Al ear problem

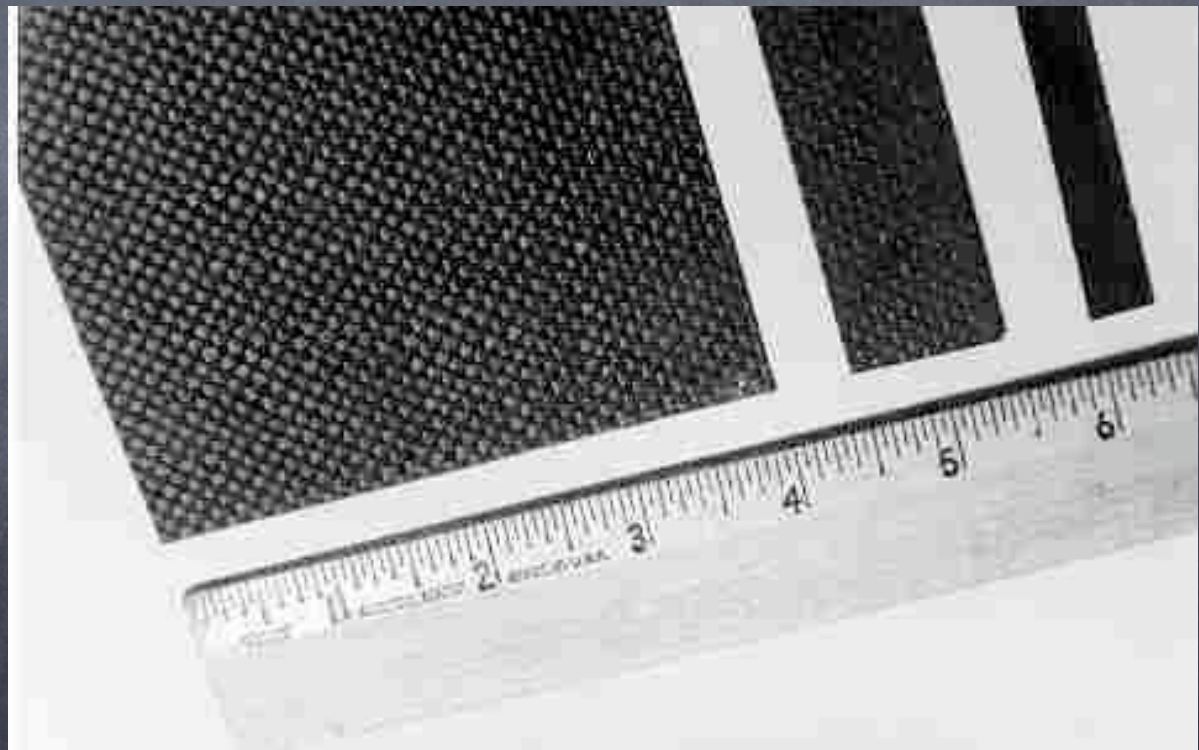


Optimized texture

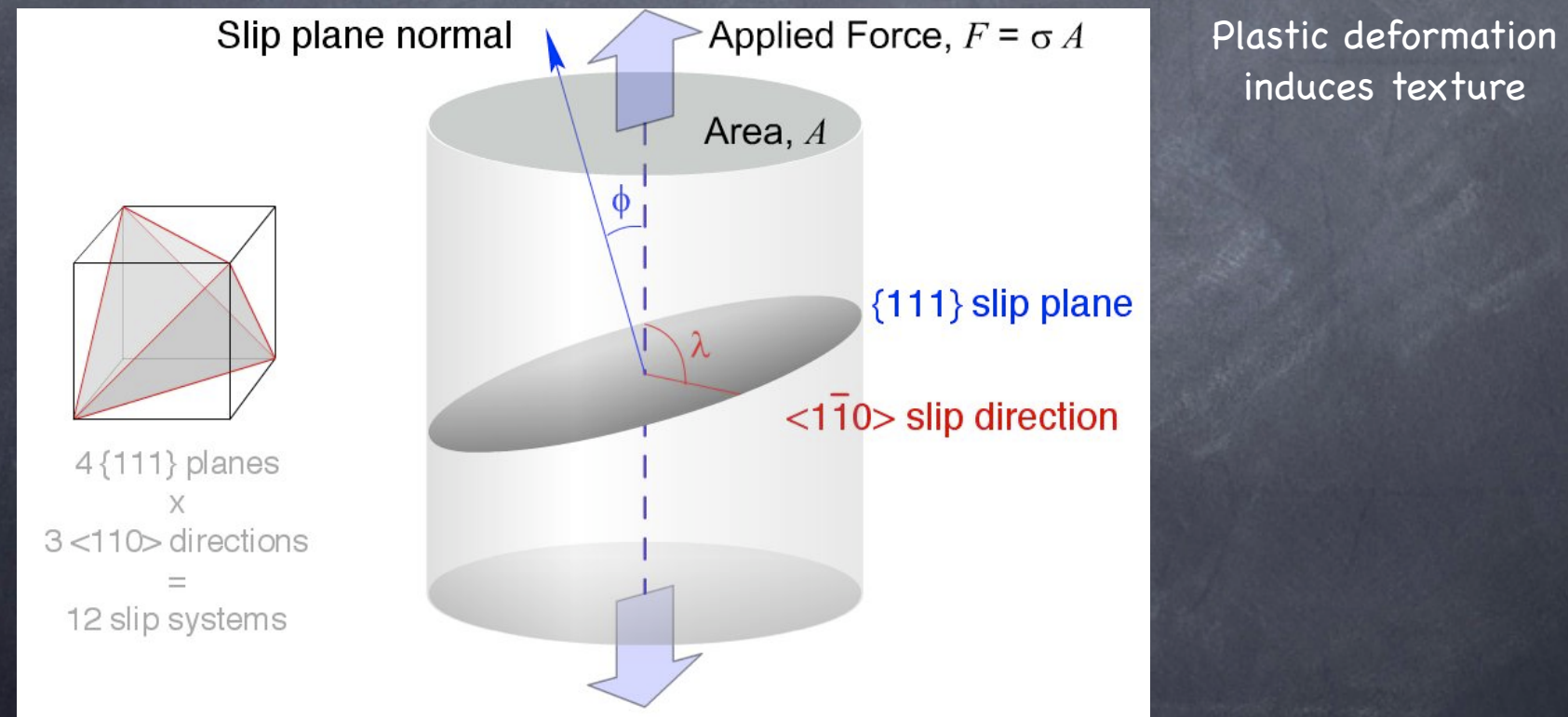
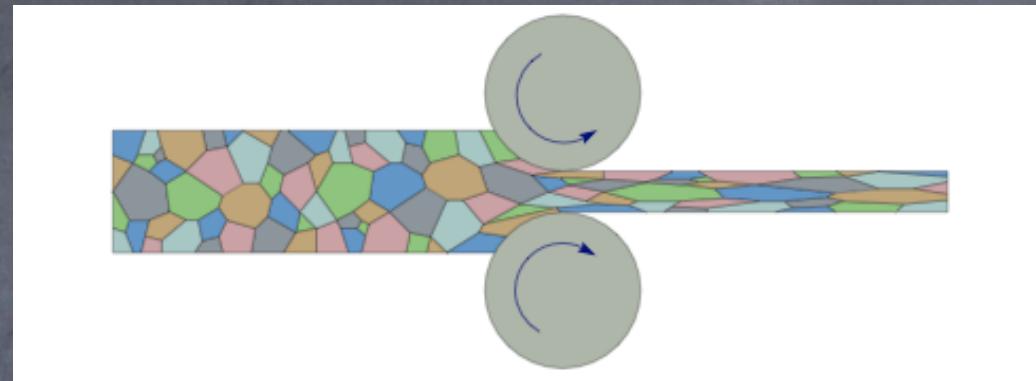
Mechanical properties

- ⌚ Stiffness
- ⌚ Strain, ultimate strain
- ⌚ Creep
- ⌚ Fracture
- ⌚ Toughness
- ⌚ Residual stresses
- ⌚

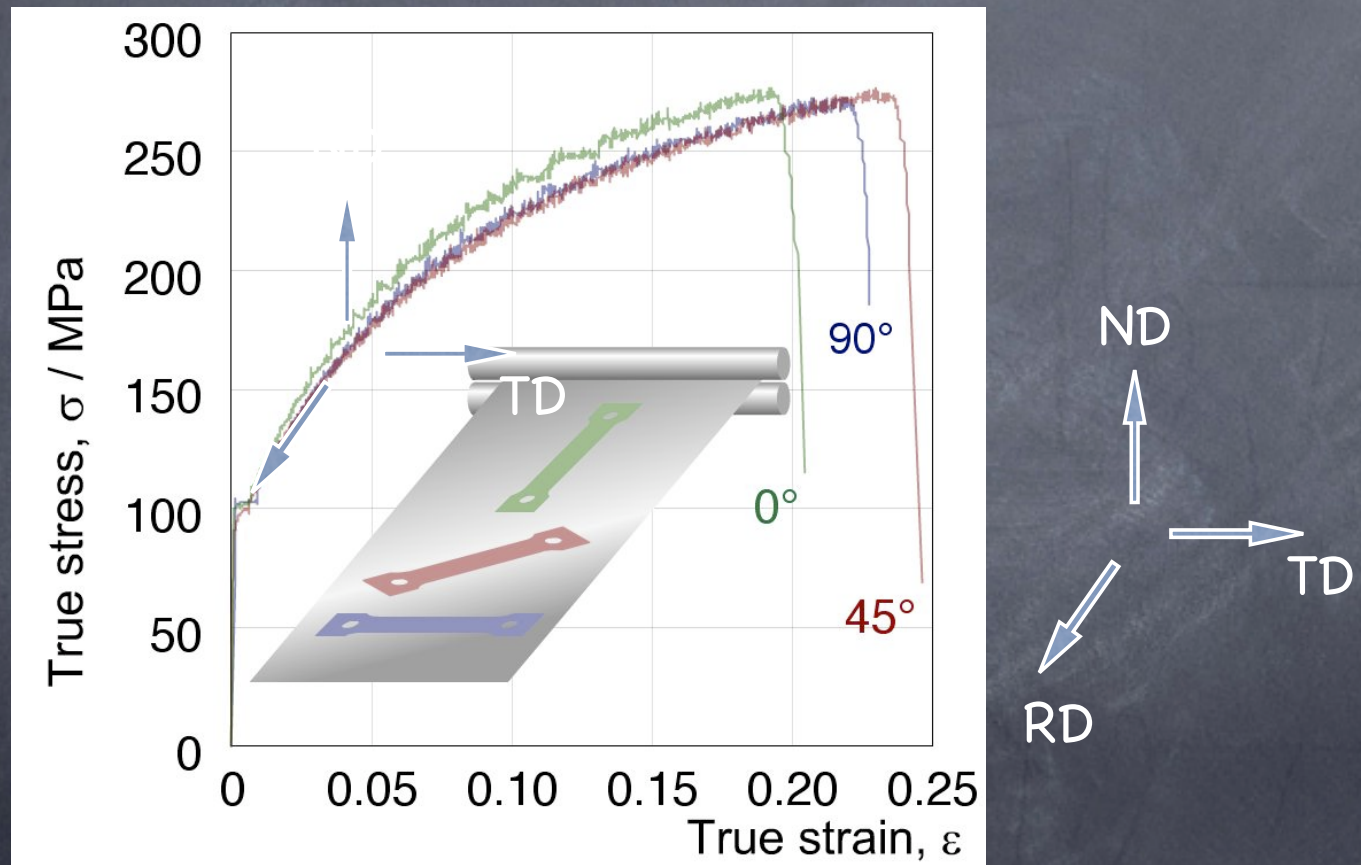
Oriented fibers, directional composites



Metals, alloys and lamination



Aluminum laminate (alloy)



Gas turbine blades

The problem: High T, creep

Material: Ni, Co superalloys

The creep is observed mainly on the grain boundary perpendicular to the applied stress



Polycrystalline blade



Directionally solidify

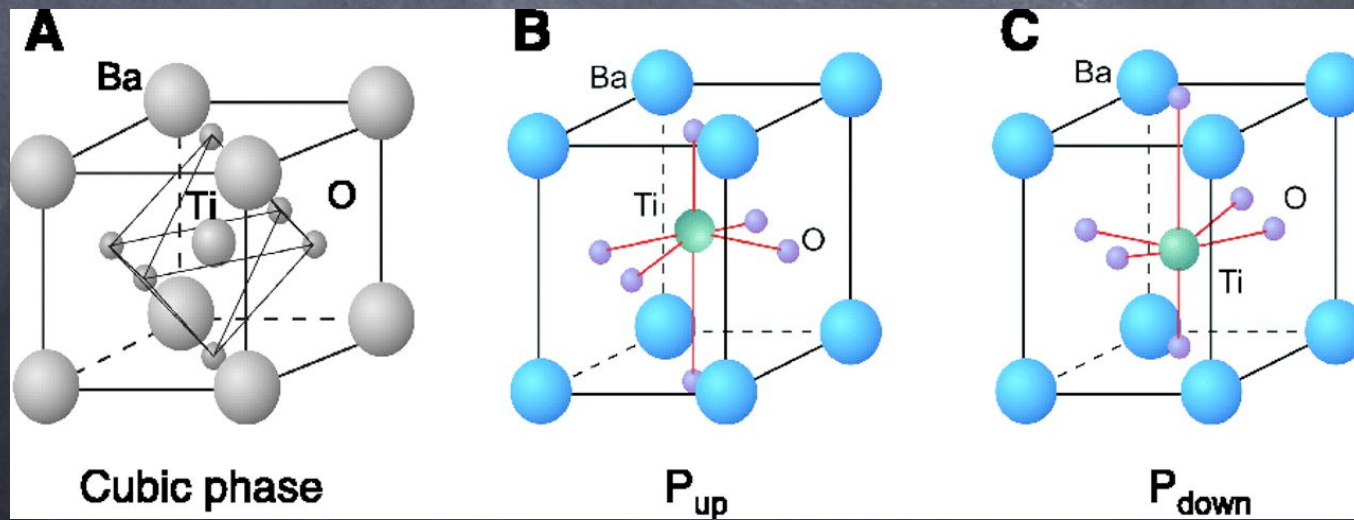


Single crystal

Electrical and magnetic properties

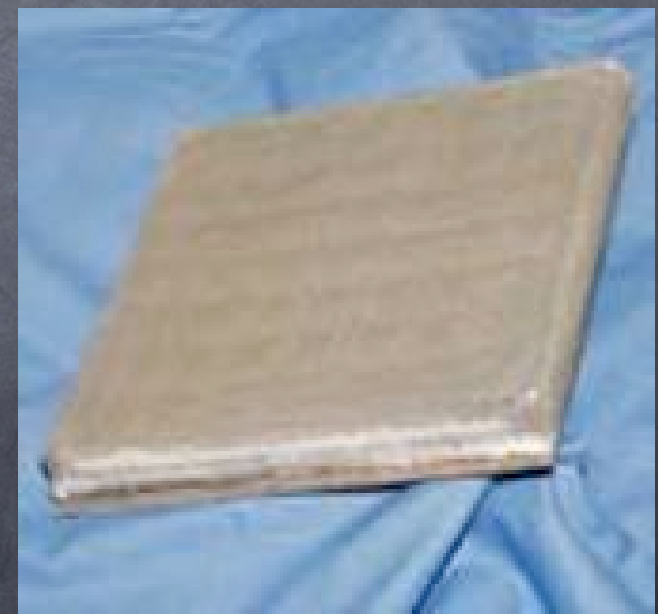
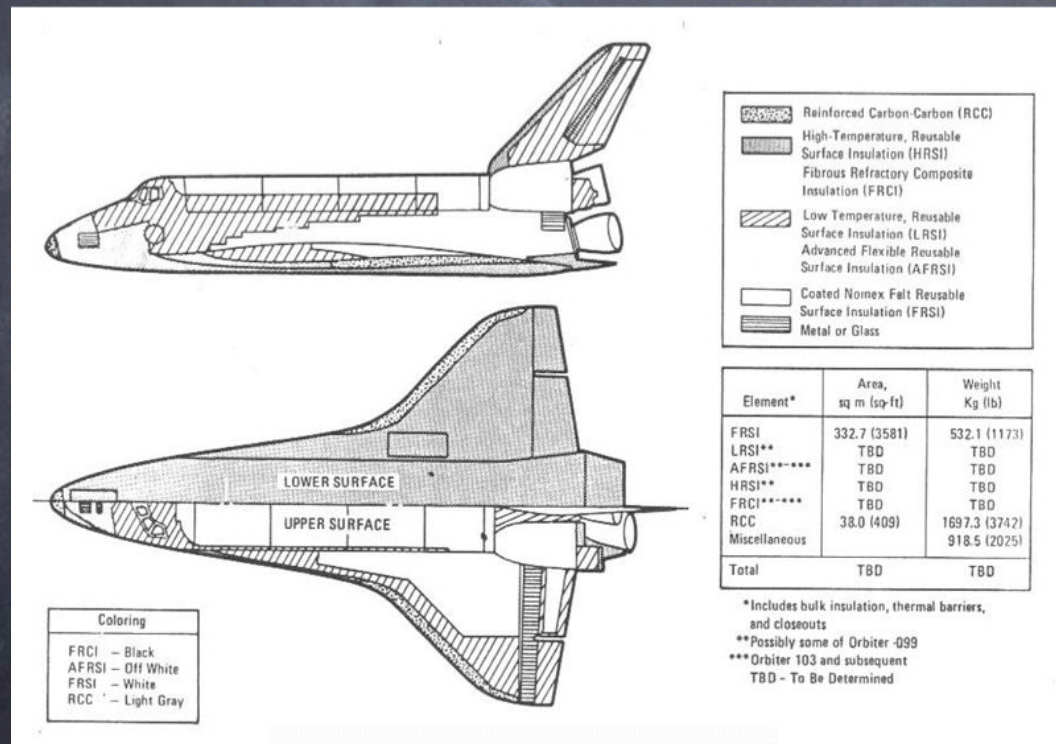
- ⦿ Superconductors
- ⦿ Semiconductors
- ⦿ Microchip, electronics
- ⦿ Magnetic cores for electrical transformer
- ⦿ Non volatile memories
- ⦿

Ferroelectrics



Anisotropic thermal properties

Shuttle TPS coating in carbon-carbon



Principles of the Rietveld method

- To minimize the residual function:

$$WSS = \sum_i w_i (I_i^{\text{exp}} - I_i^{\text{calc}})^2, w_i = \frac{1}{I_i^{\text{exp}}}$$

- where:

$$I_i^{\text{calc}} = S_F \sum_k L_k |F_k|^2 S(2\theta_i - 2\theta_k) P_k A + bkg_i$$

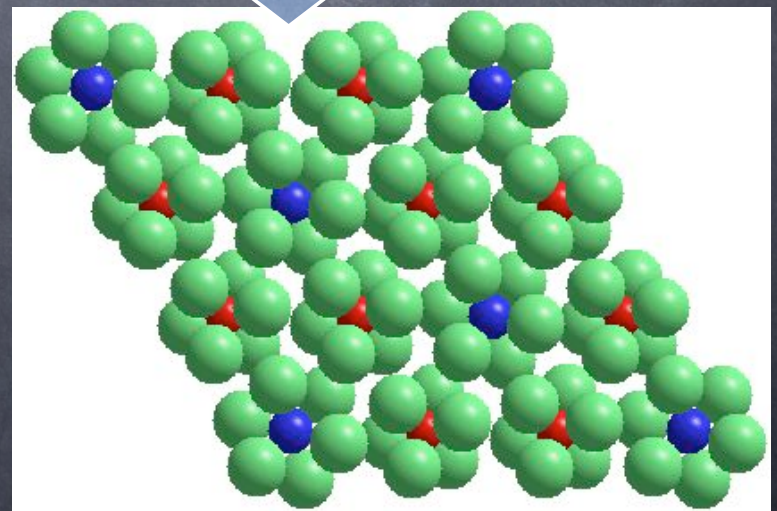
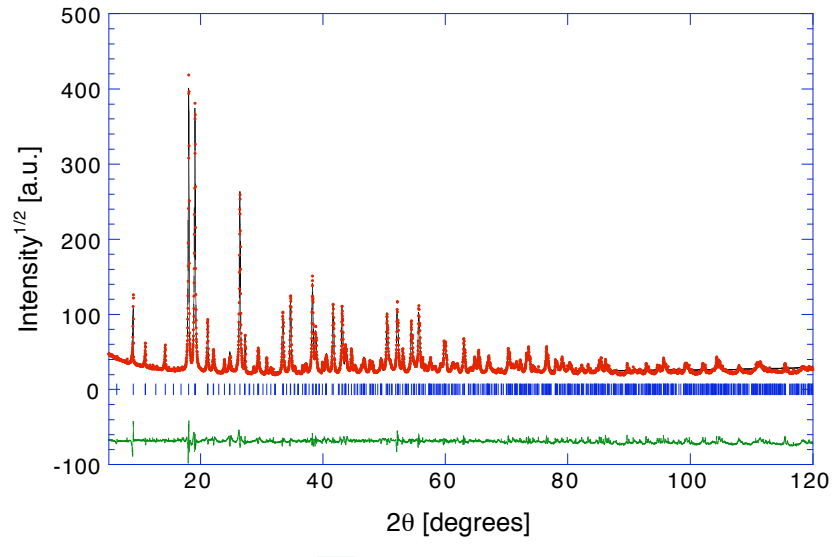
P_k = preferred orientation function

$S(2\theta_i - 2\theta_k)$ = profile shape function

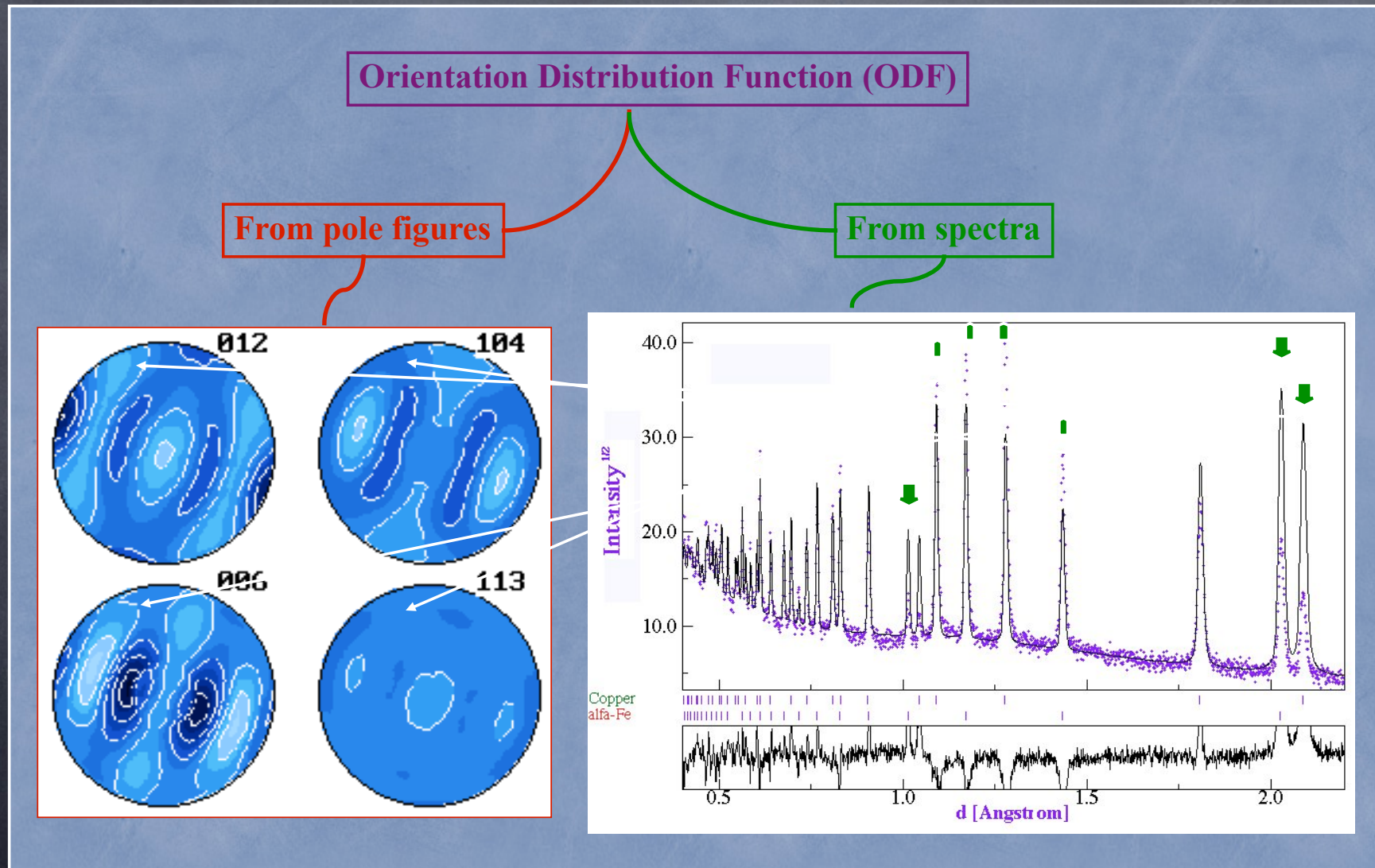
(PV : η , HWHM)

$$\text{HWHM}^2 = U \tan^2 \theta + V \tan \theta + W$$

$$P_k = \left(r^2 \cos^2 \alpha + \frac{\sin^2 \alpha}{r} \right)^{-3/2}$$



Texture from Spectra



How it works (RiT A)

- The equation:

$$I_i^{calc}(\chi, \phi) = \sum_{n=1}^{N_{phases}} S_n \sum_k L_k |F_{k;n}|^2 S(2\theta_i - 2\theta_{k;n}) P_{k;n}(\chi, \phi) A + bkg_i$$

- Harmonic:

$$P_k(\chi, \phi) = \sum_{l=0}^{\infty} \frac{1}{2l+1} \sum_{n=-l}^l k_l^n(\chi, \phi) \sum_{m=-l}^l C_l^{mn} k_n^{*m}(\Theta_k \phi_k)$$

$$f(g) = \sum_{l=0}^{\infty} \sum_{m,n=-l}^l C_l^{mn} T_l^{mn}(g)$$

- Clmn are additional parameters to be refined

- Data (reflections, number of spectra) sufficient to cover the odf

- Advantages:

- Easy implementation
- Very elegant, completely integrated in the Rietveld
- Fast, low memory consumption to store the odf.

- Disadvantages:

- No automatic positive condition ($ODF > 0$)
- Not for sharp textures
- Low symmetries \rightarrow too many coefficients to refine (where are the advantages?)
- Memory hog for refinement.

How it works (RiTA)

• WIMV

- Discrete method. ODF space is divided in regular cells (ex. 5x5x5 degrees) and the function value is stored for each cell.

- Numerical integration:

-

- For each refinement cycle:

- P_k extracted (Le Bail method)
- ODF computed (WIMV or EWIMV)
- P_k recalculated
- Fitting of the spectra

- Advantages:

- $ODF > 0$, always
- Ok for sharp textures and low symmetries

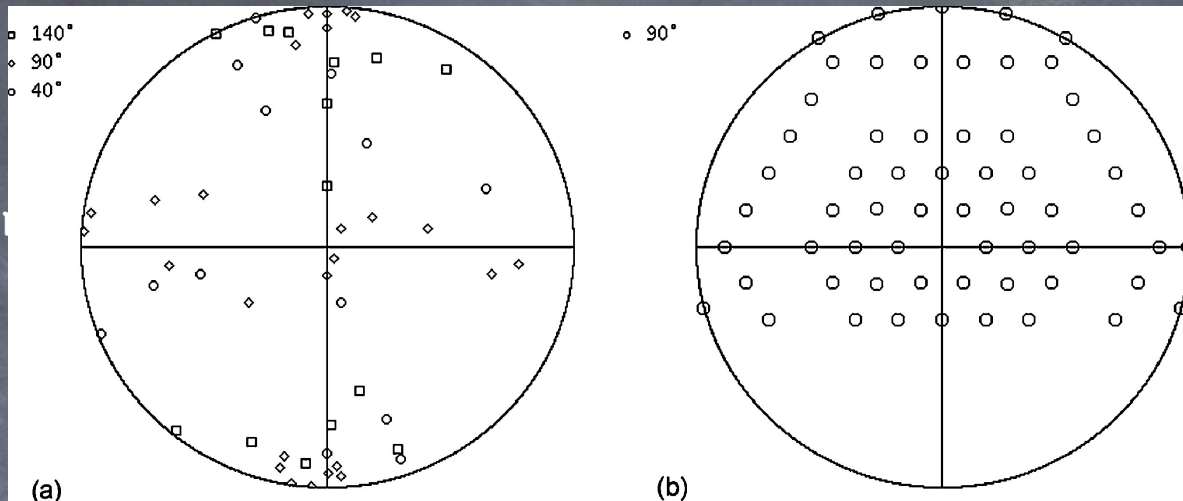
- Disadvantages:

- Less elegant (require extraction and interpolation to a regular grid)
- Trickly for implementation
- ~~slower~~

$$P_k(\chi, \phi) = \int f(g, \varphi) d\varphi$$

Why neutron?

- A early '90 round better for texture (920-927, 1991)



- The good:

- depth of penetration + relatively big neutron beam = good statistics for large grain samples
- Debye-Scherrer like geometry = coverage in the pole figure up to 90° possible

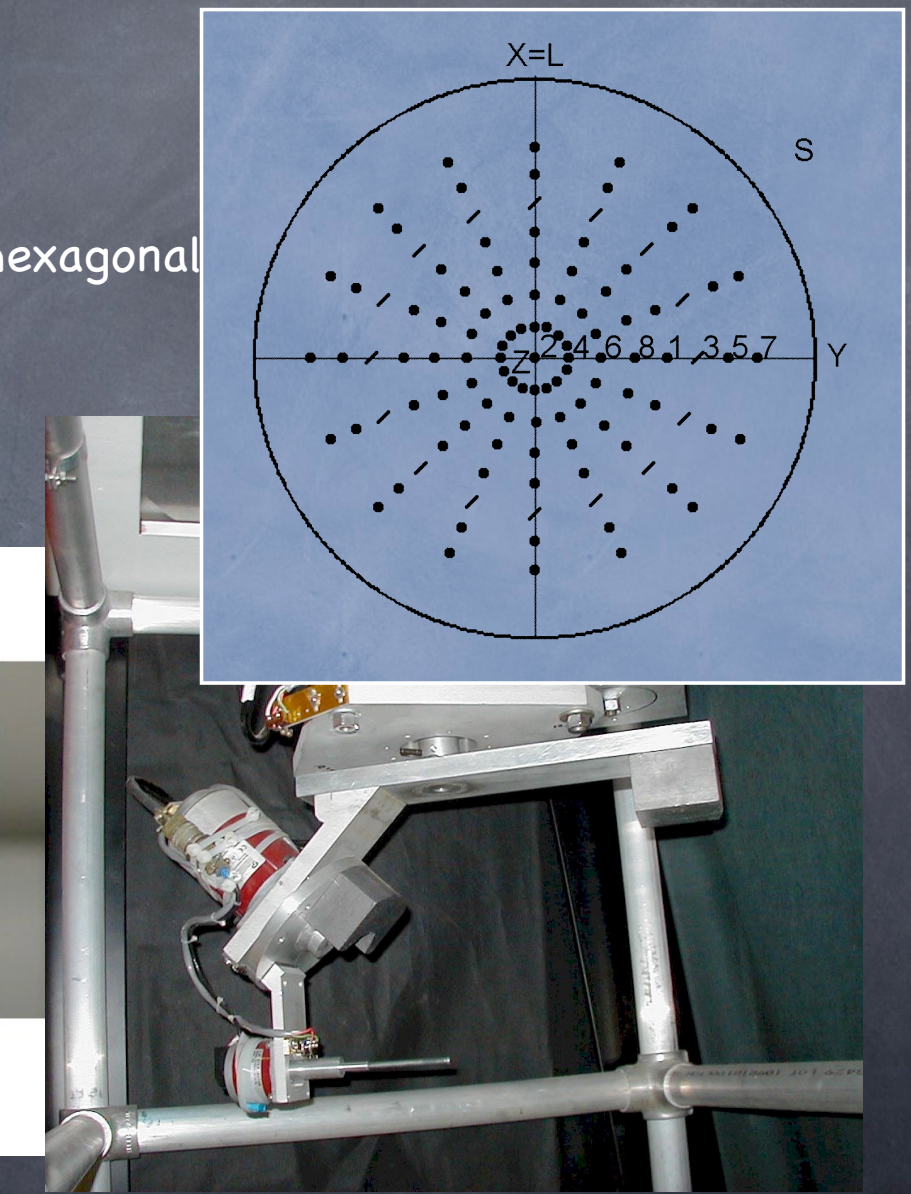
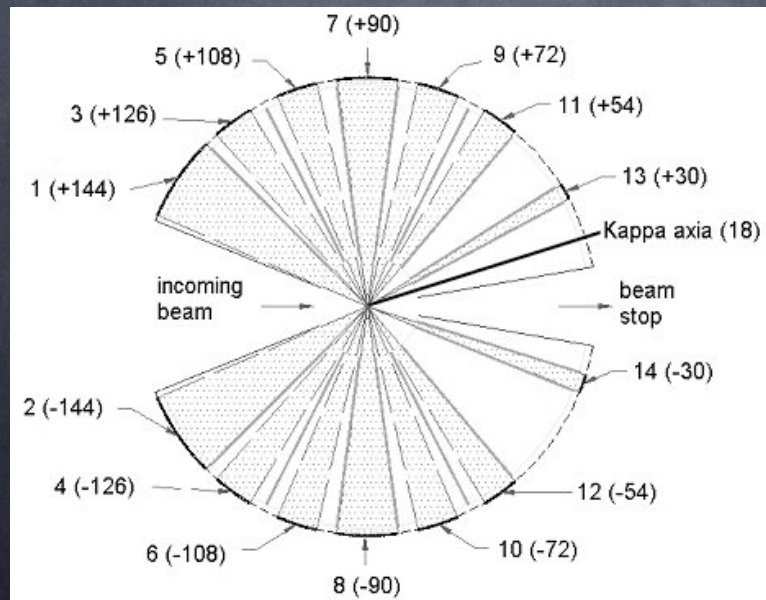
- The bad:

- resolution (intensity is needed first), in progress
- availability (multi-detector machine, position sensitive), in progress

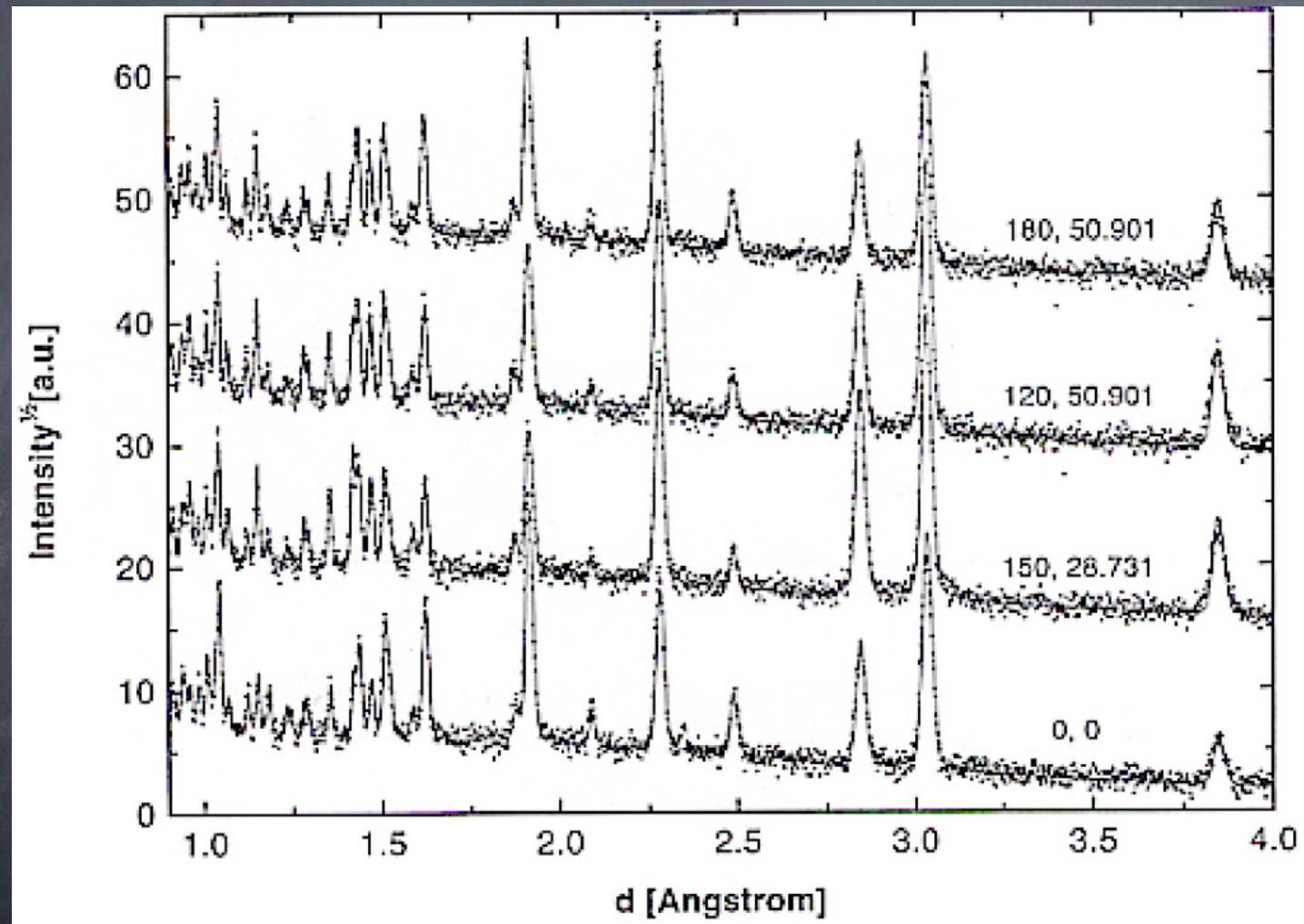
Limestone standard analysis (first test)

With H.-R. Wenk and S. Matthies

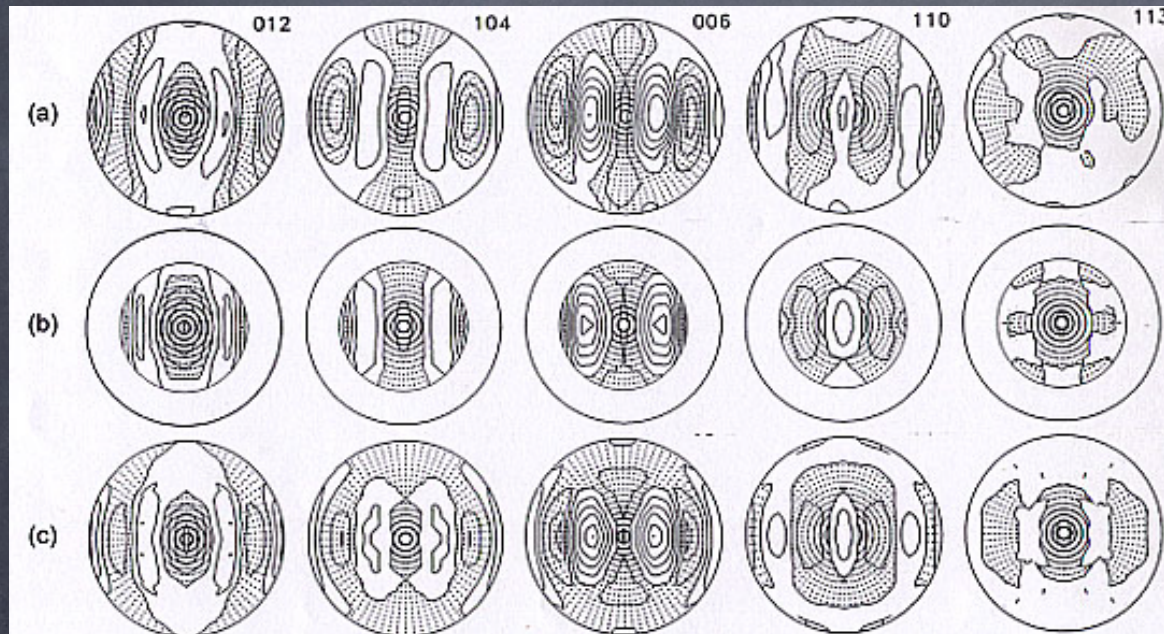
- Data collected at IPNS (GPPD)
- Neutron TOF, kappa goniometer, hexagonal bank (only one quarter)



TOF spectra fitted for Limestone (some)



Limestone: experimental and reconstructed pole figures



ILL round robin

Extracted PFs

Recalculated PFs

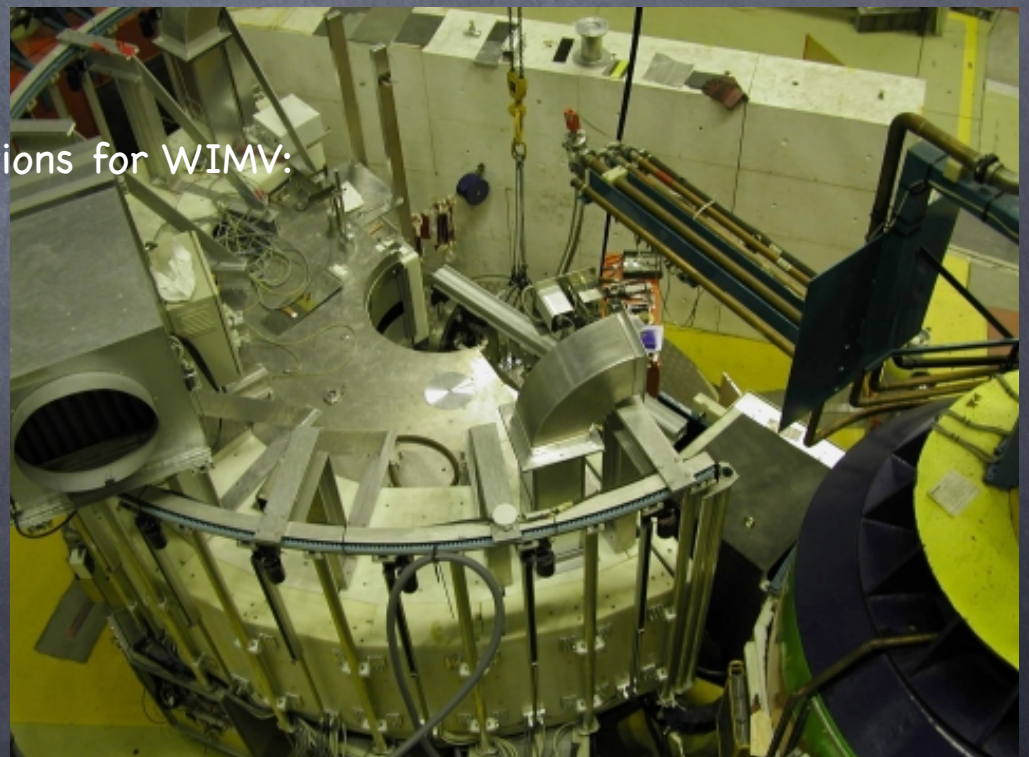
Limestone: new measurements at ILL

Measurement

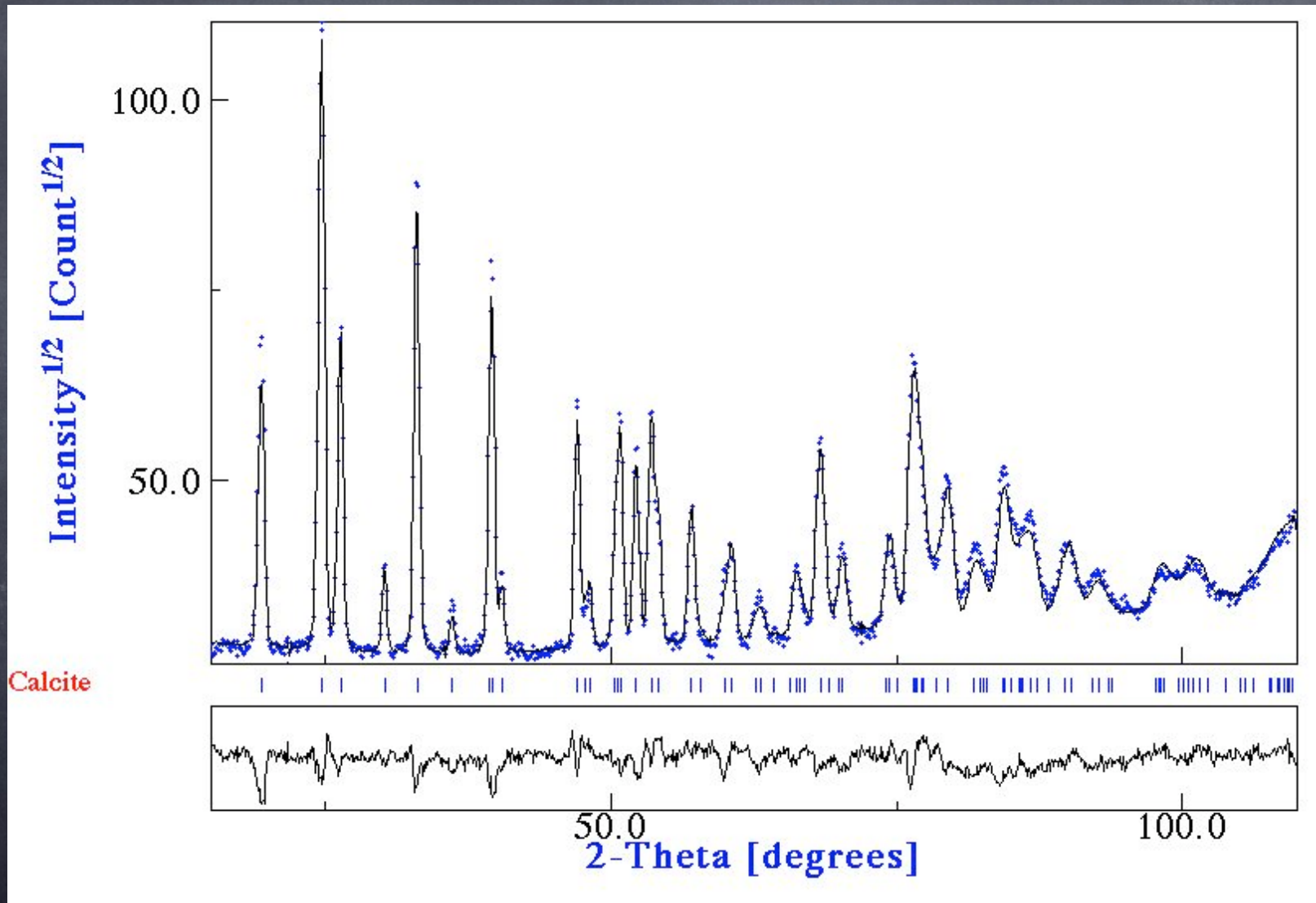
- Spectra collection at the D20 beamline at ILL (Grenoble, T. Hansen, D. Chateigner); high intensity beamline.
- Two ω positions (50° and 142°) of the Eulerian cradle; $5^\circ \times 5^\circ$ resolution in χ and ϕ .

Analysis

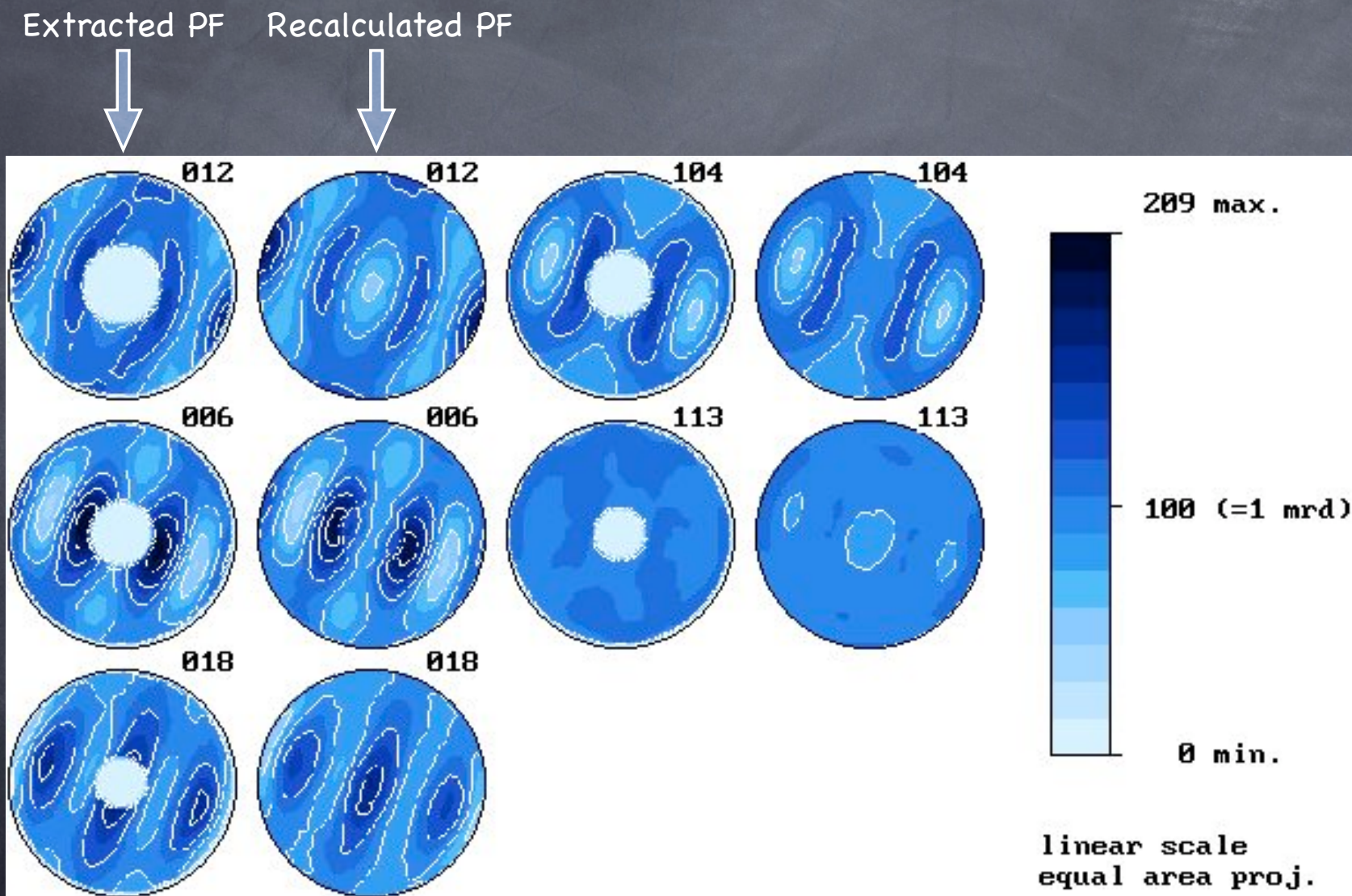
- Only one ω position (142°) used and $10 \times 10^\circ$ resolution (number of datafiles reduced to 1/8, 360).
- No sample symmetries assumed.
- Two criteria for reflection selections for WIMV:
 - Peak intensity > 20% highest
 - Peak intensity > 10% highest



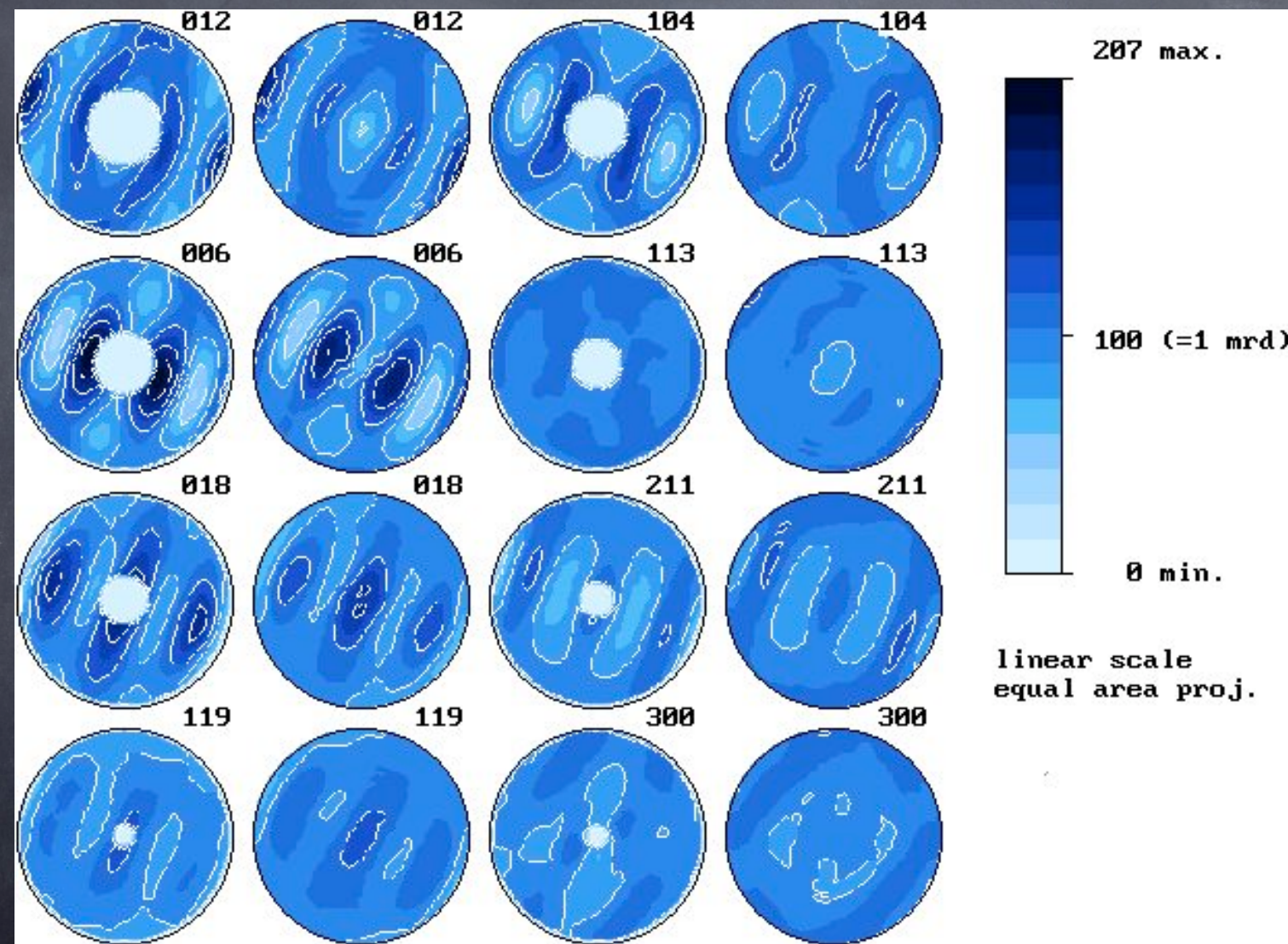
One of the spectra fitted



Limestone (ILL): extracted and reconstructed pole figures



Limestone (ILL): more pole figures used



Limestone IPNS vs. ILL results

- IPNS limited by the faster measurement and only one quarter of PF coverage
- Using more reflections for WIMV results in a smoother ODF; less agreement with the extracted PFs
- Only one ω position ($10^\circ \times 10^\circ$ grid) sufficient for texture determination.
- Crystal structure refinement equivalent

The metamorphic quartzite

With S. Matthies and K. Ullmeyer

- Sample:

- Clast from a metaconglomerate in Wildrose Canyon (Death Valley National Park, California)
- Cylindrical sample, 2 cm diameter for 2 cm long

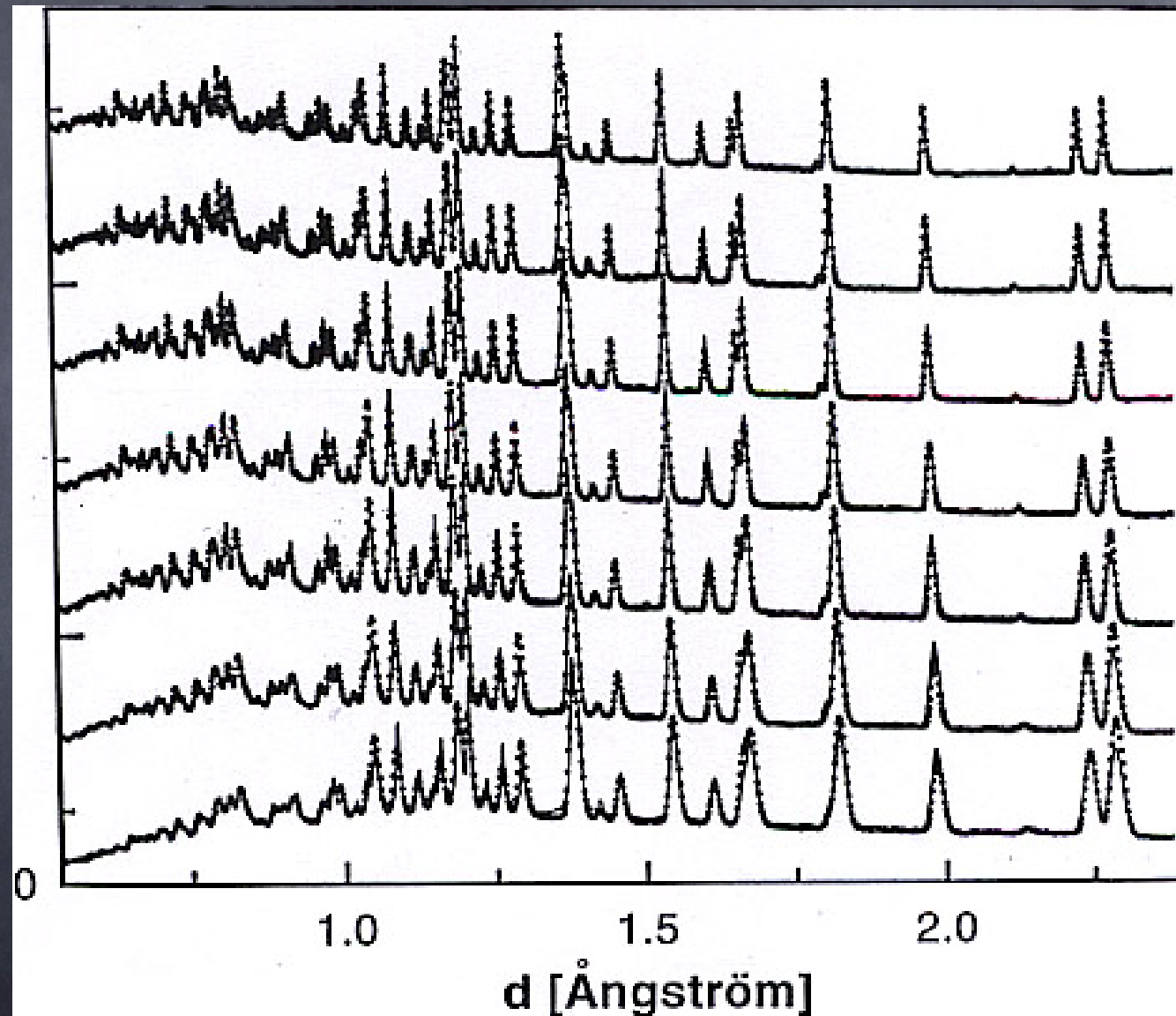
- Data collection:

- Neutron TOF at JINR-Dubna (pulsed reactor IBR-2) (K. Ullmeyer)
- 7 detectors at two different positions and one axis sample rotation lead to 650 spectra at the constant grid resolution of 7.2° (15 minutes for each position).

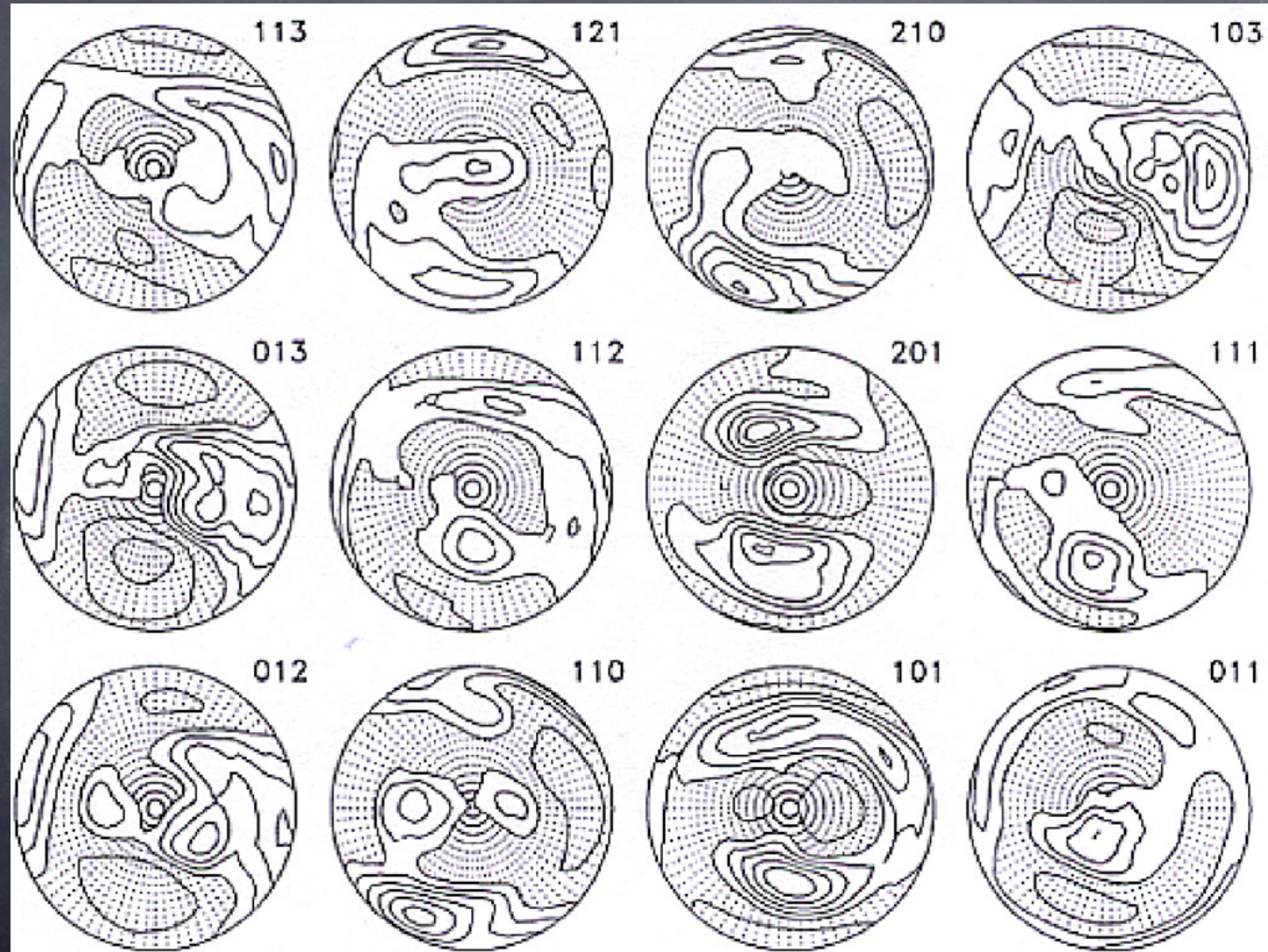
- Analysis:

- Analysed range of 0.5-3.5 Angstrom (527 reflections)
- Only 301 spectra used (to reduce memory consumption)
- Only reflections stronger than 10 % (and 5 %) of the strongest were used for texture analysis corresponding to 37 reflections (62).
- Crystal structure of α -Quartz assumed

Quartzite TOF spectra fitted (some)



quartzite reconstructed PFs



Quartzite results

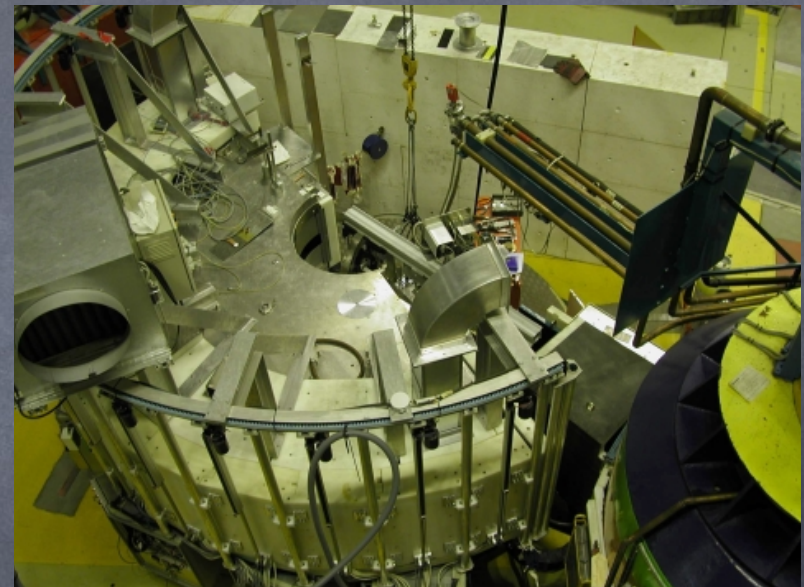
- Using 62 peaks instead of 37 for texture analysis did not show remarkable improvements
- Agreement between the ODF so determined and the optical measurements
- Crystal structure refinement

Space Group	a [Angstrom]	c [Angstrom]	Si (x,x,0)	B _{Si} [Angstrom ²]	O (x,y,z)	B _O [Angstrom ²]
P3 ₂ 1	4.91393(5)	5.40394(9)	0.46323(7)	0.4(2)	0.41047(5) 0.26474(5) 0.78471(3)	0.7(1)

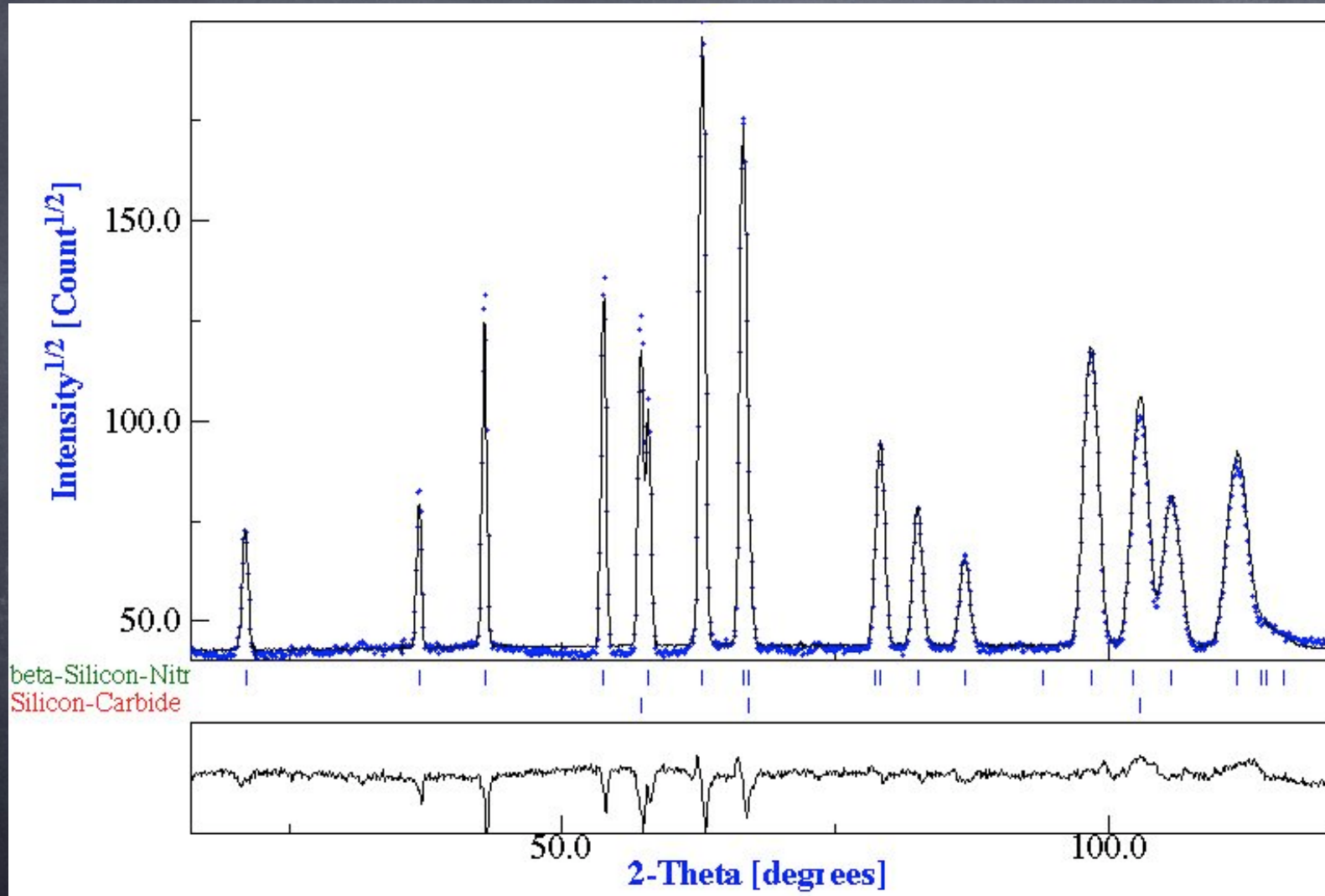
Analysis of Composites: Si₃N₄+SiC

With D. Chateigner and T. Hansen

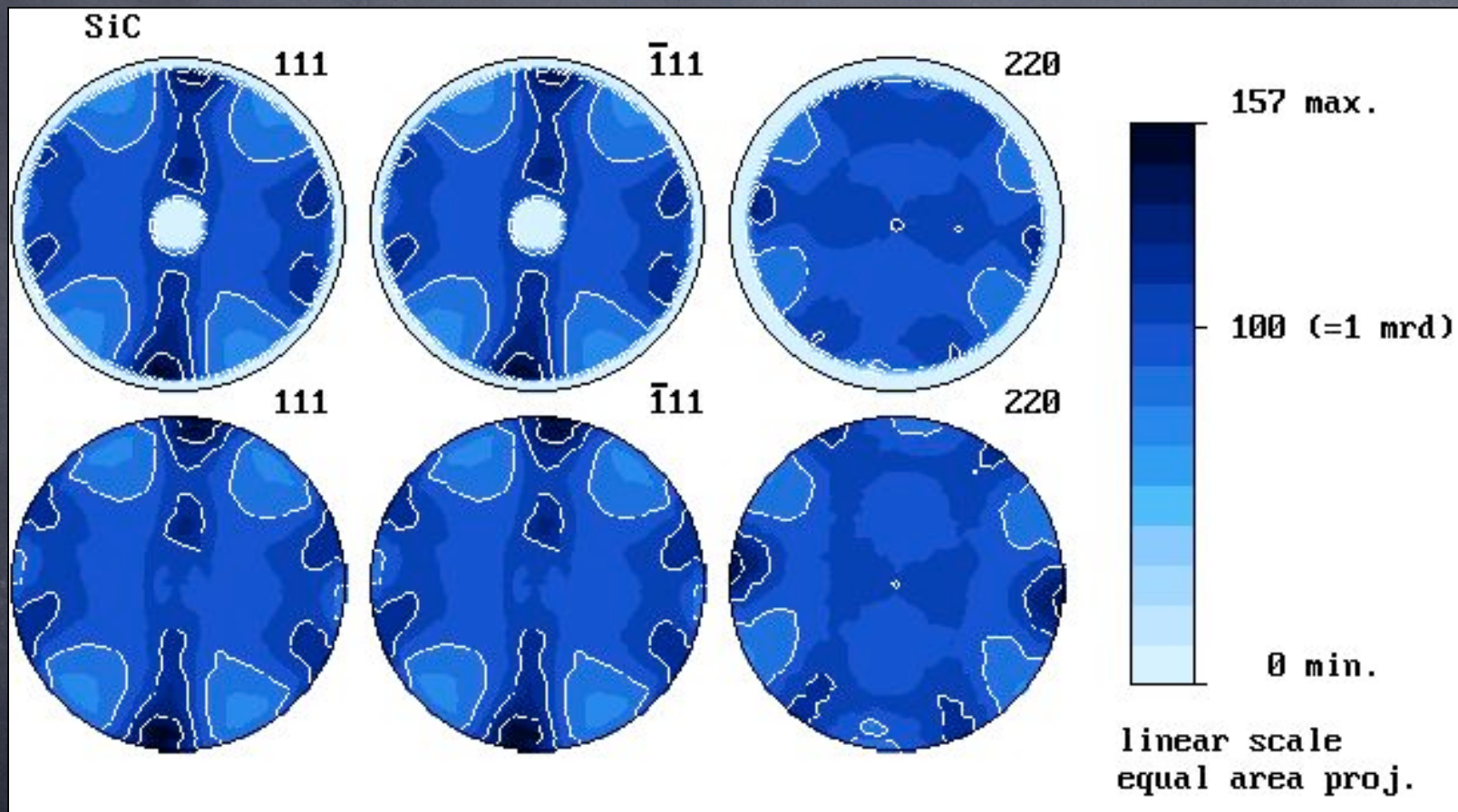
- ⦿ SiC whiskers: (111) along fiber direction
- ⦿ Matrix: β -Si₃N₄
- ⦿ Minor glass quantity (for sintering aid)
- ⦿ Composite obtained by HIP
- ⦿ Diffraction measurements:
 - ⦿ D20-ILL: neutron, PSD, Eulerian cradle
 - ⦿ 720 spectra, $10^\circ \times 10^\circ$ grid on χ and ϕ , 2 ω positions
 - ⦿ Analyzed by Maud using RiTA (Rietveld Texture Analysis)



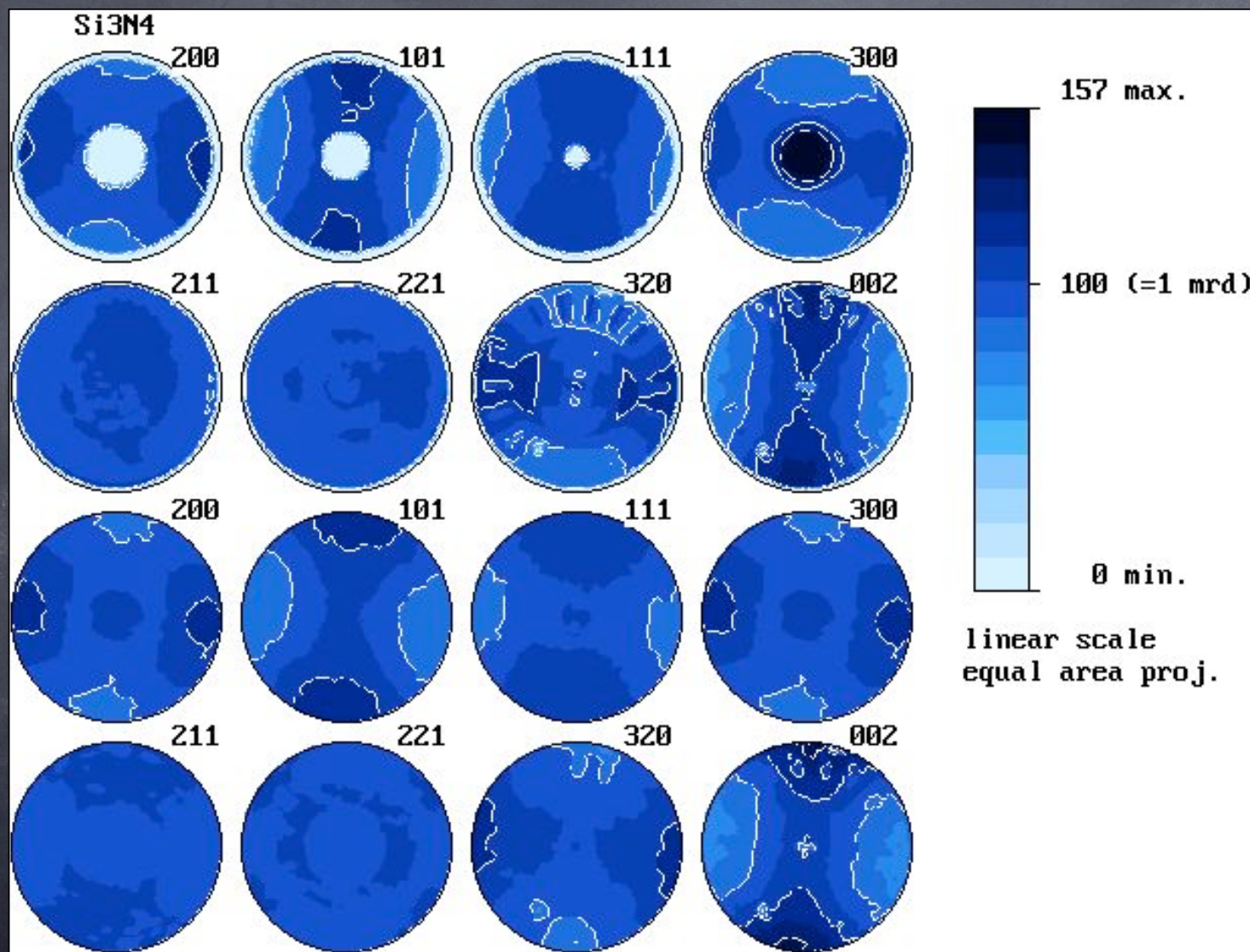
Fitting the spectra



SiC whiskers pole figures



Si_3N_4 : experimental and reconstructed pole figures



Kryptonite results

- ⦿ SiC distributed mainly in the basal plane of the composite
 - ⦿ Optimum in plane mechanical properties of the composites
- ⦿ β -Si₃N₄ has a random ODF
- ⦿ SiC volume fraction: 24.2 %

Ötzi e la metallurgia alpina del rame

- ✓ Le asce in rame erano oggetti di culto o venivano utilizzate nel lavoro/caccia quotidiano?
- ✓ L'approccio "materialistico": si studia il processo di produzione/lavorazione delle asce per individuare la destinazione d'uso
- ✓ Metodo: studio della tessitura cristallografica tramite analisi non distruttive

L'ascia di Ötzi/Icemen, 3200 a.C.



Altre asce della zona prealpina (31 tot)



Lovere, Bergamo - LOV 330



Bocca Lorenza, Vicenza BL-162415



Remedello, Brescia - Tomba 62

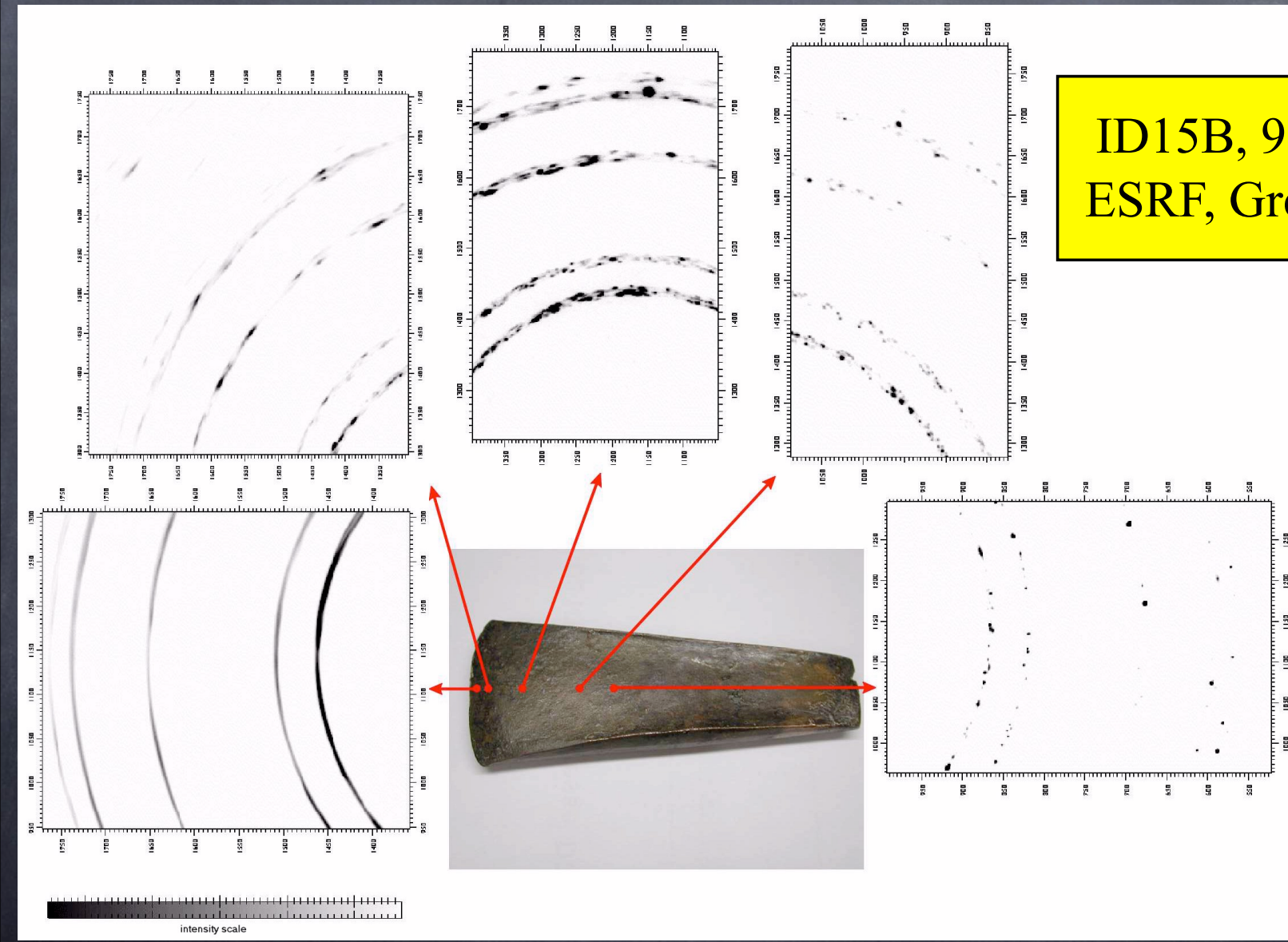


Remedello, Brescia - Tomba 102



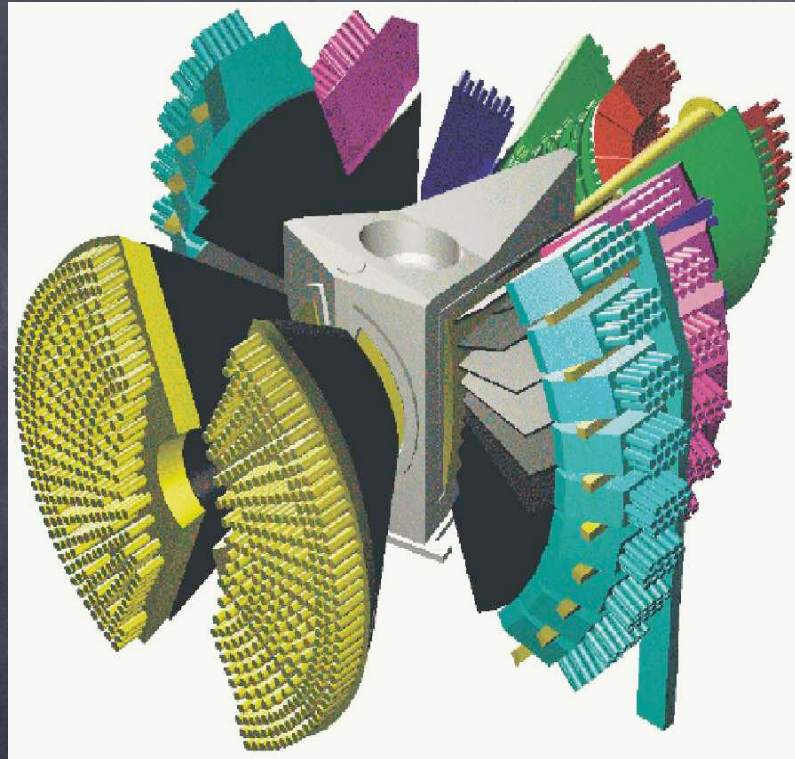
Gamertinerhof/Castelrotto

Analisi metallografica non distruttiva, sincrotrone alta energia



ID15B, 90KeV
ESRF, Grenoble

Analisi tessitura (diffrazione neutronica)

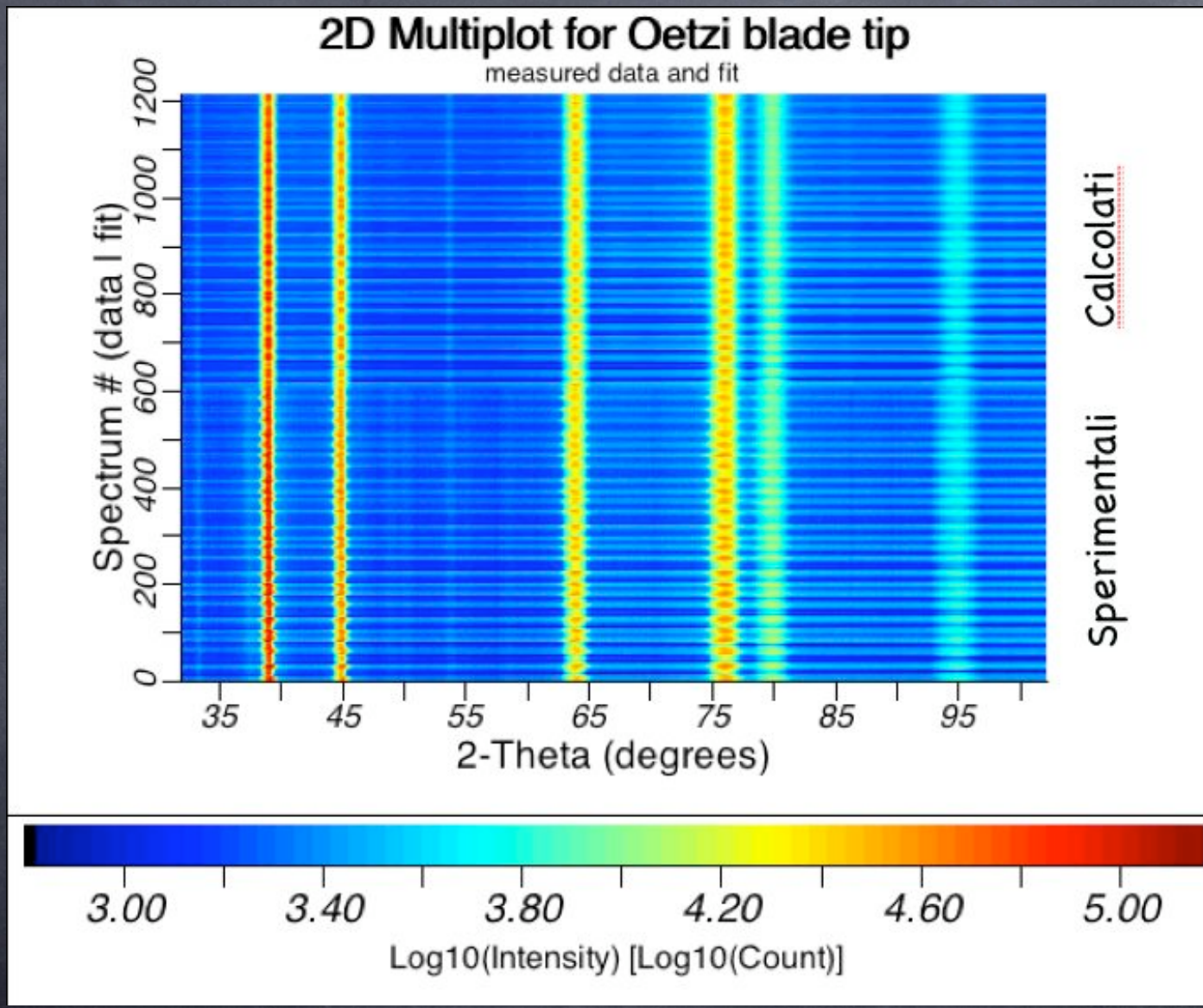


ISIS - GEM & Rotax
Oxford, UK

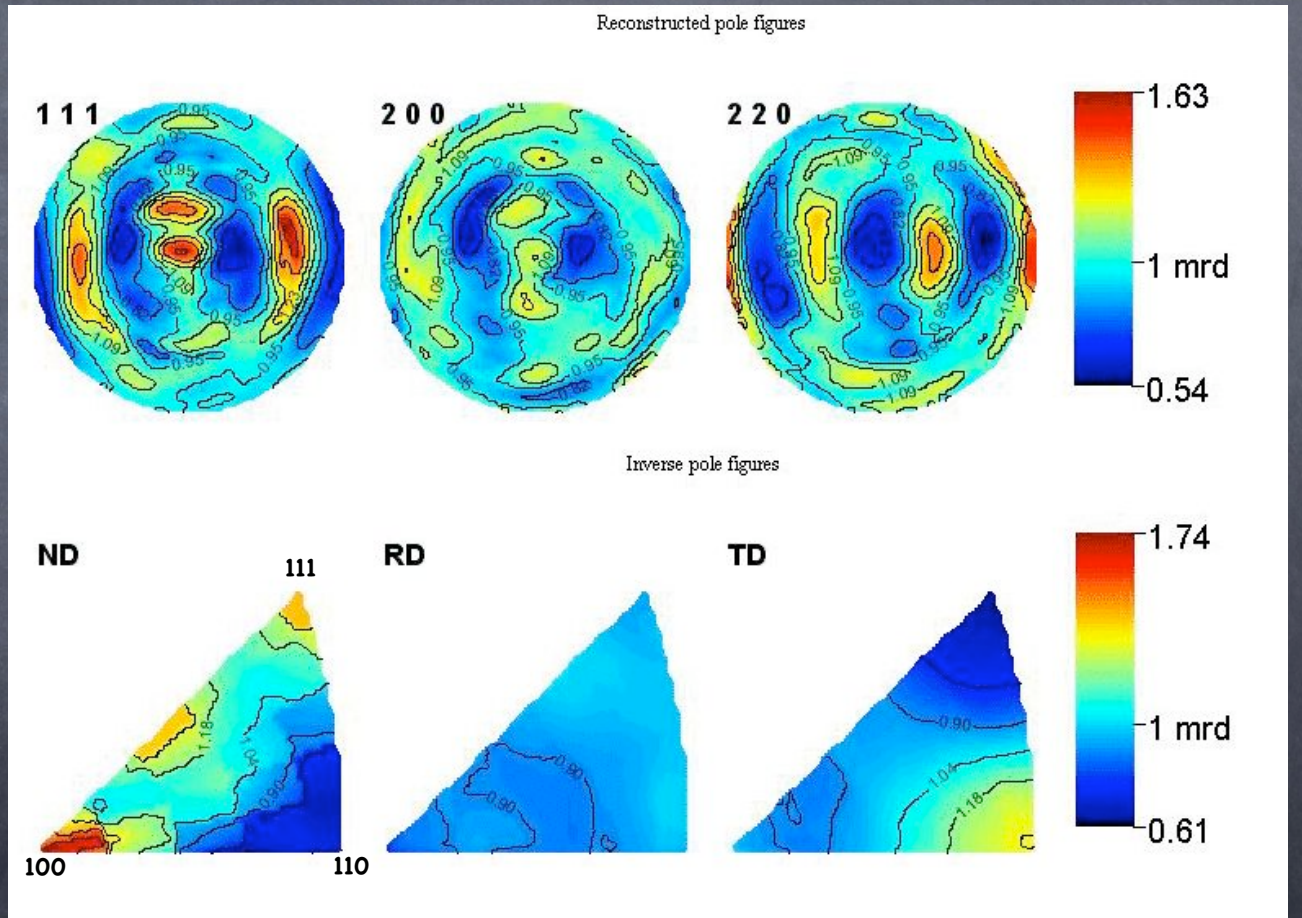
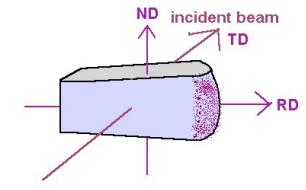


ILL – D20
Grenoble, F

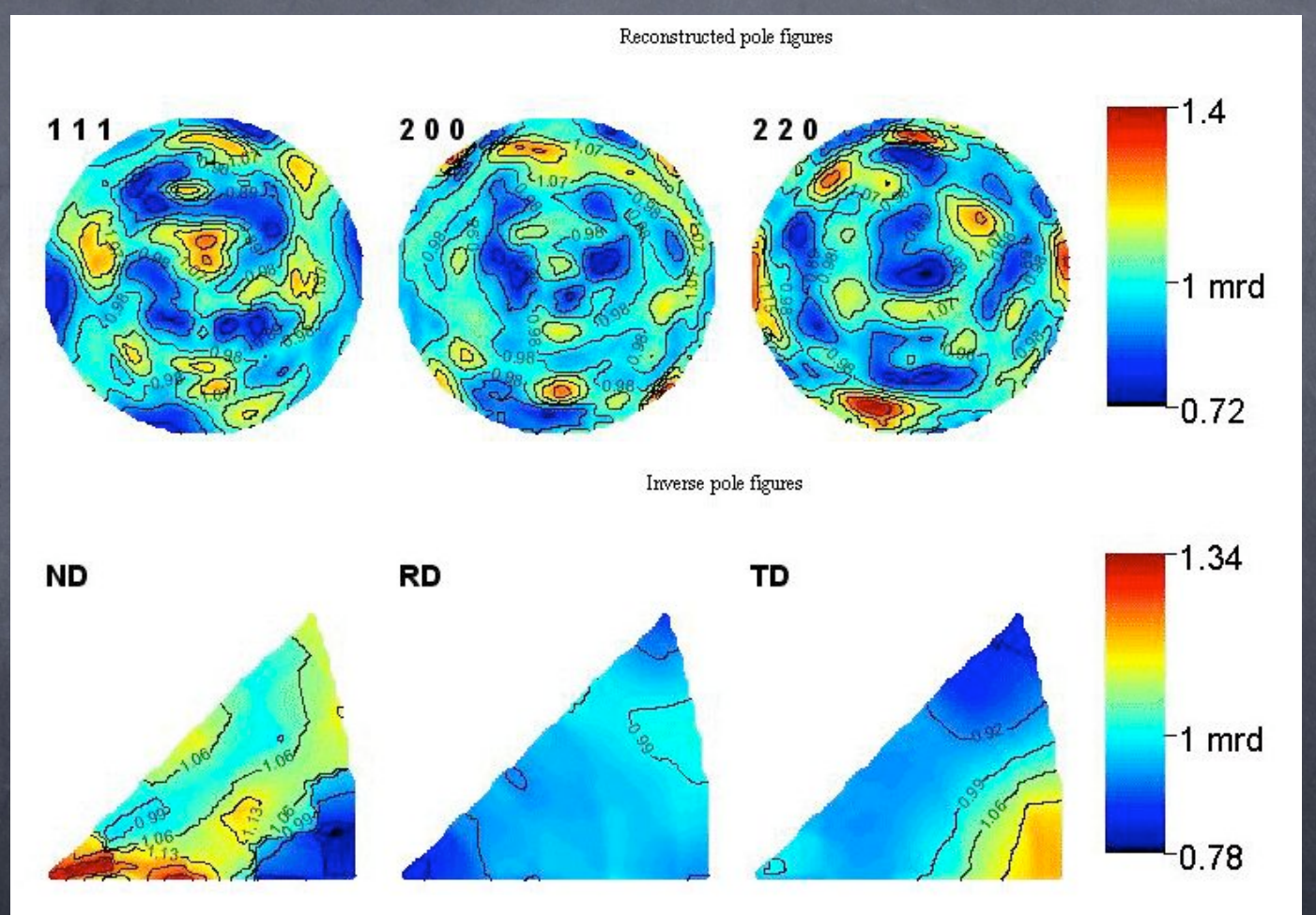
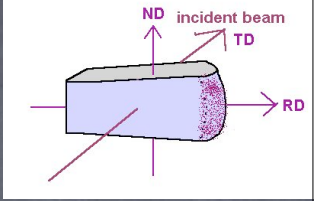
Alcuni spettri di diffrazione



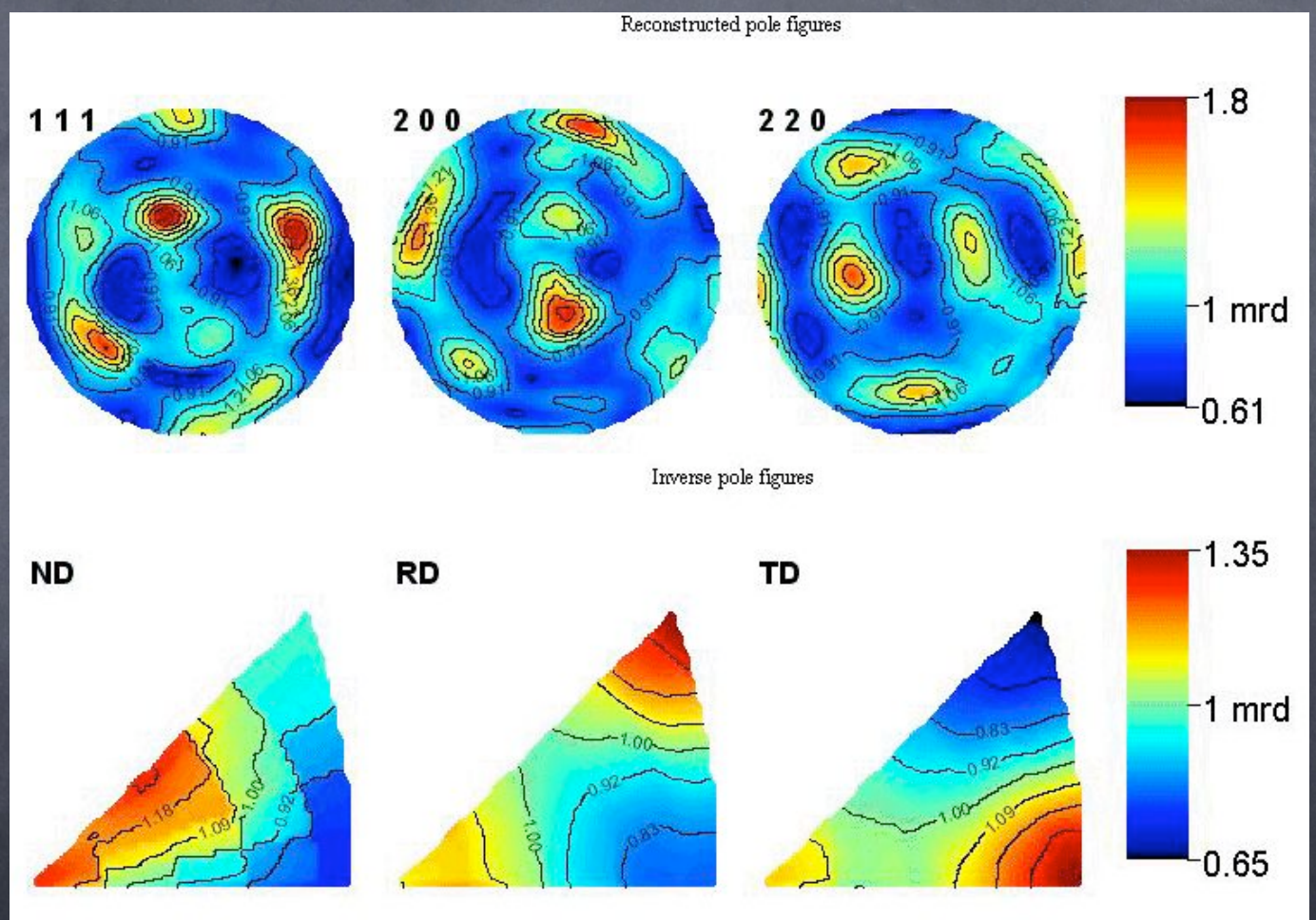
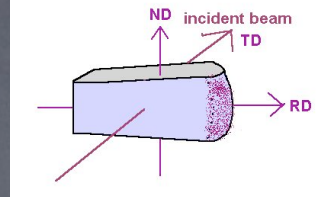
Lovere LOV-330 (rolling texture)



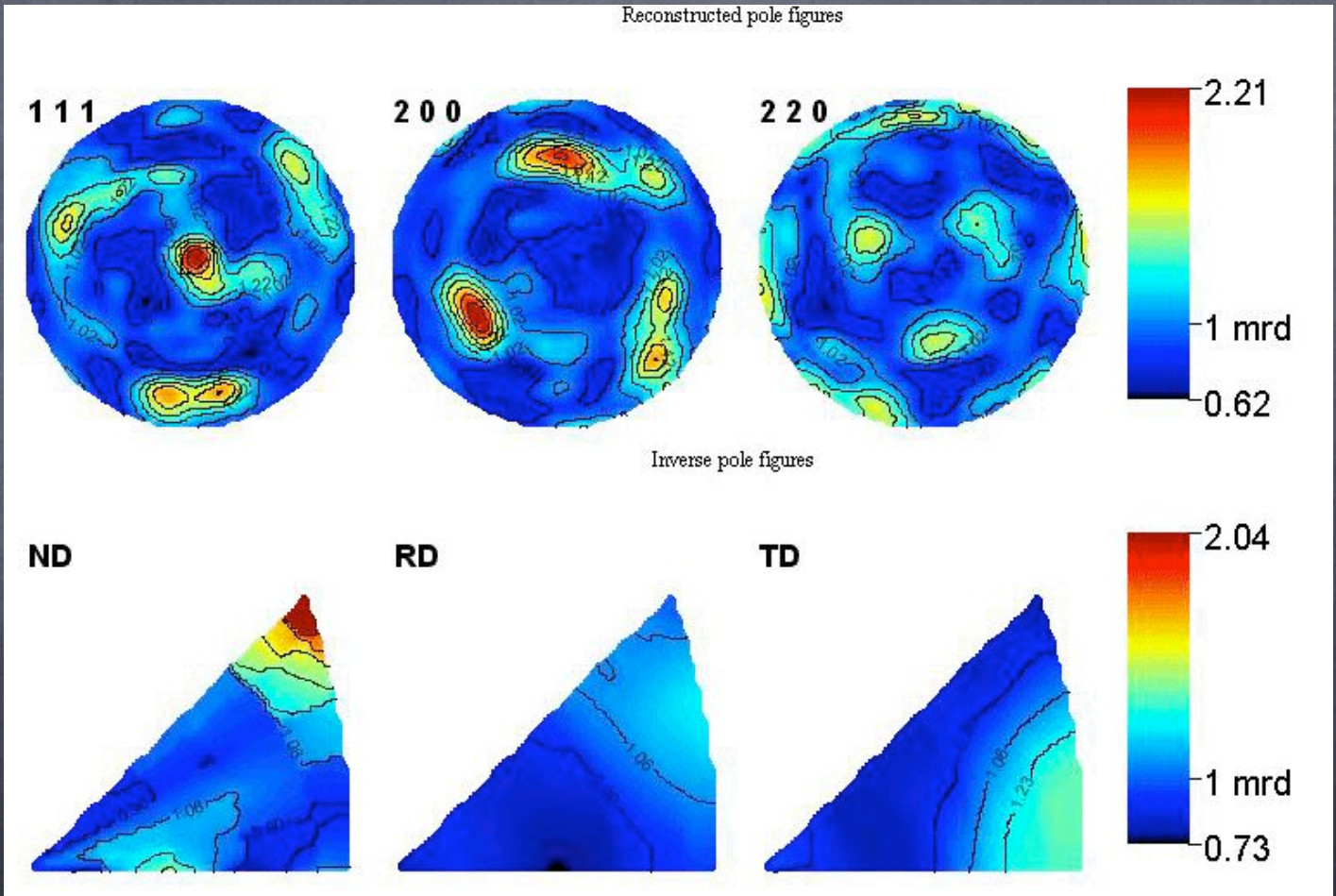
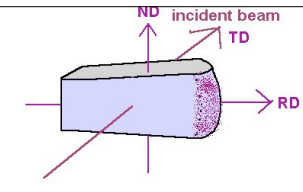
Remedello, tomba 102 (Rolling, ricristallizzato)



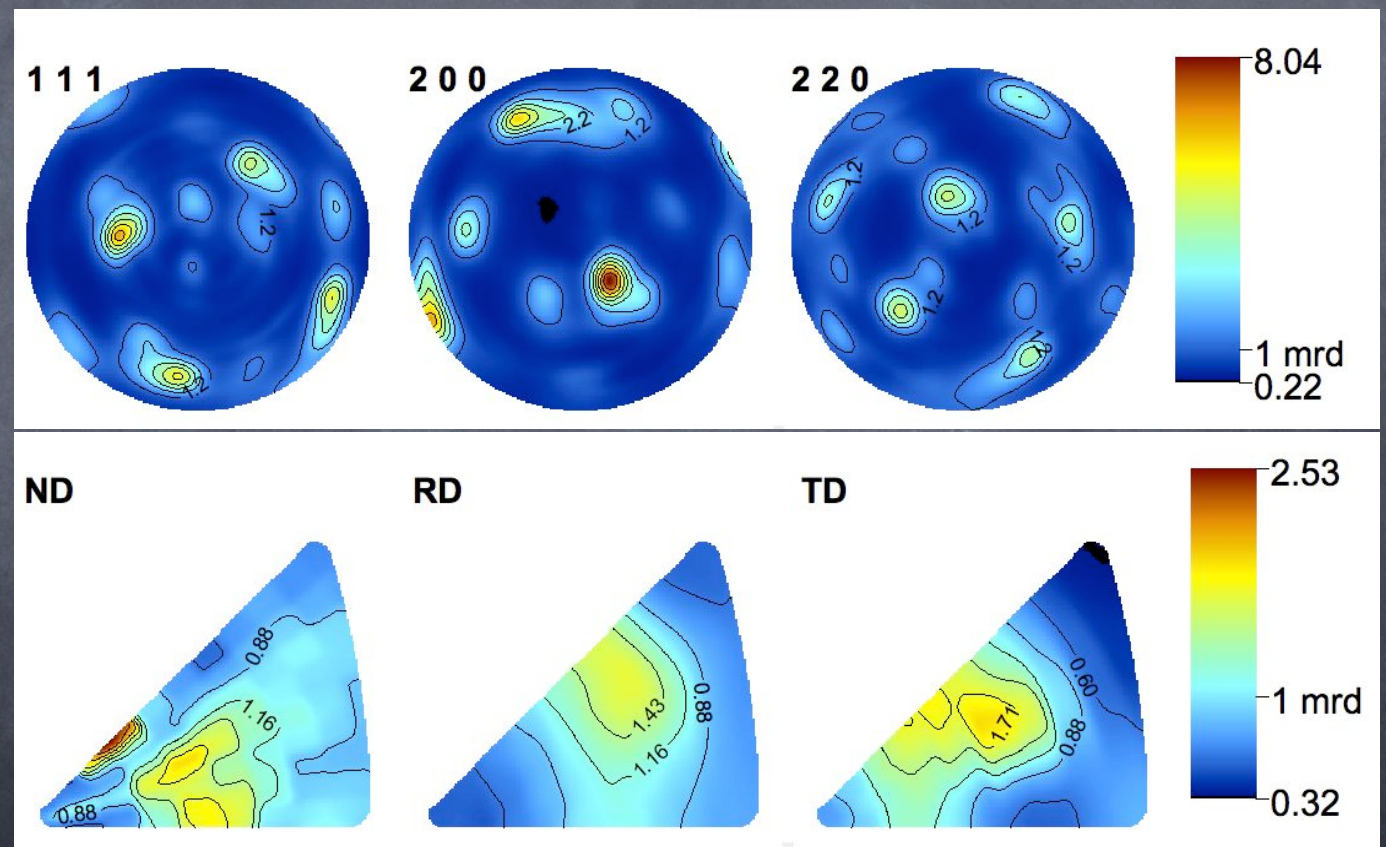
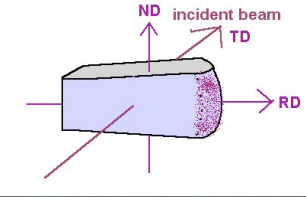
Bergamo, LS-238 (cube texture)



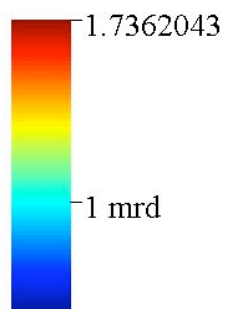
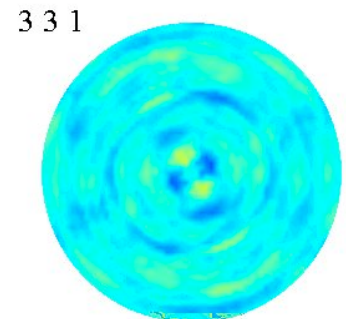
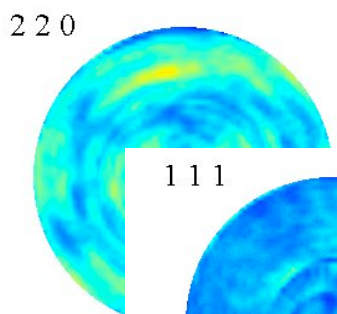
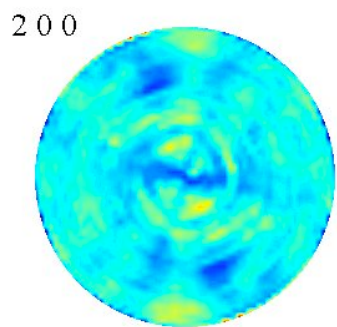
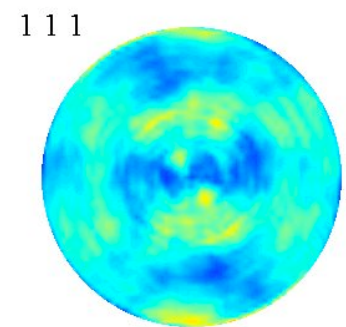
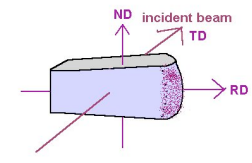
Hirzlsteig (Compression/cube)



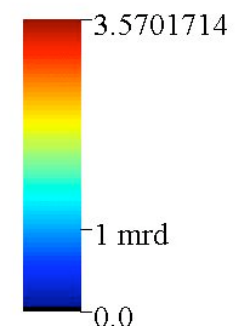
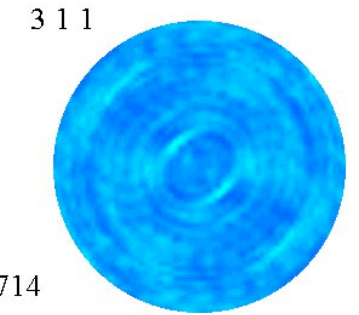
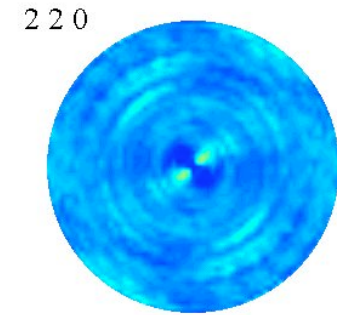
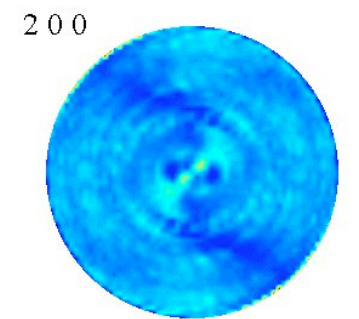
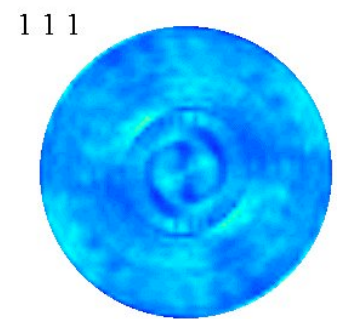
Gamertinerhof Castelrotto (cube texture)



Icemen/Ötzi (no texture)



Lama



Centro ascia

Conclusioni asce (preliminari)

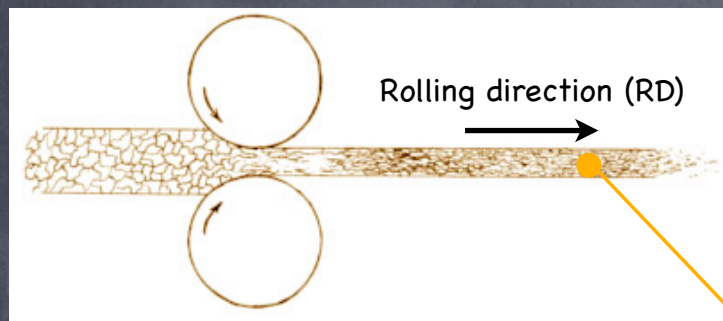
- ✓ Alcune asce mostrano una cube texture tipica di un processo ripetuto di battitura e ricristallizzazione (stato finale ricotto).
- ✓ Alcune asce invece mostrano battitura e poca ricristallizzazione (più incrudite), ma forse meno utilizzate.
- ✓ L'ascia di Otzi è allo stato "as cast". Solo alcuni indicazioni di battitura sul bordo della lama (si tratta di ascia cerimoniale?)

Da evitare, solo analisi non distruttive

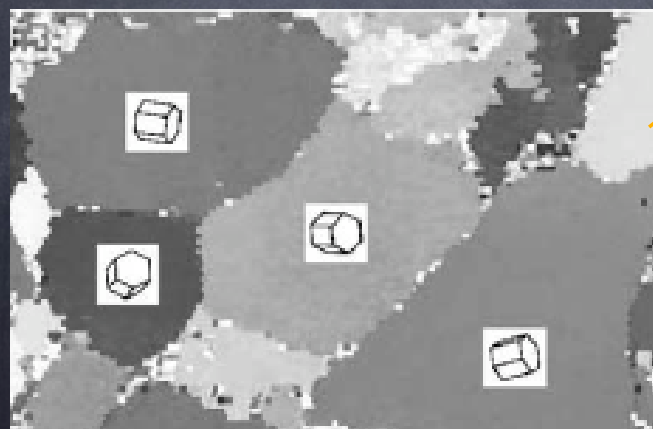
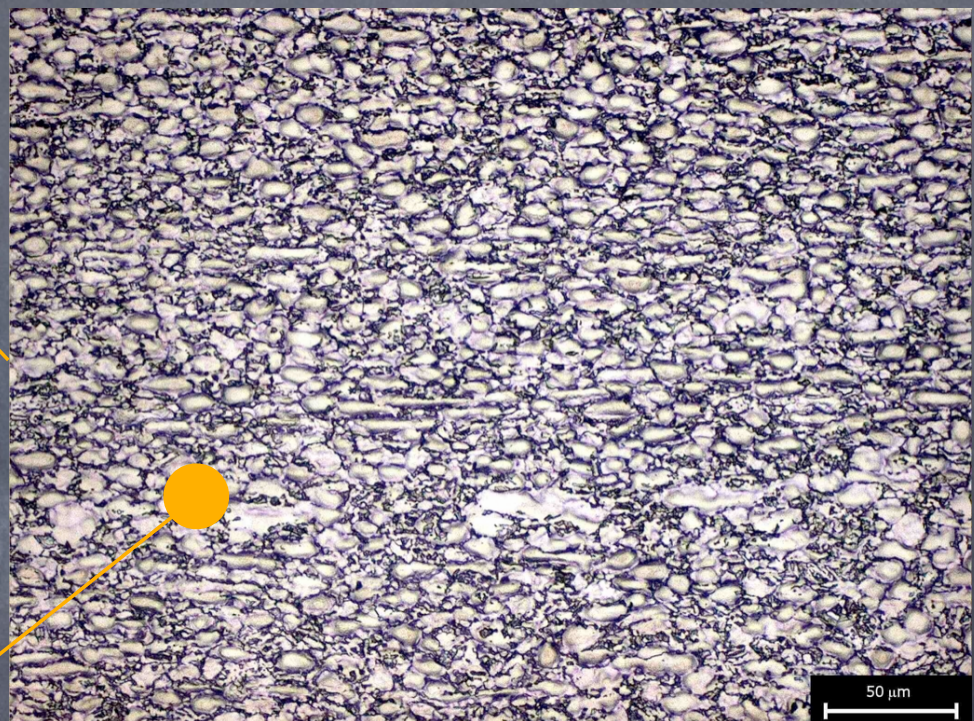


Texture and memory effects in metals

With H. -R. Wenk and I. Lonardelli



Ti 6Al 4V



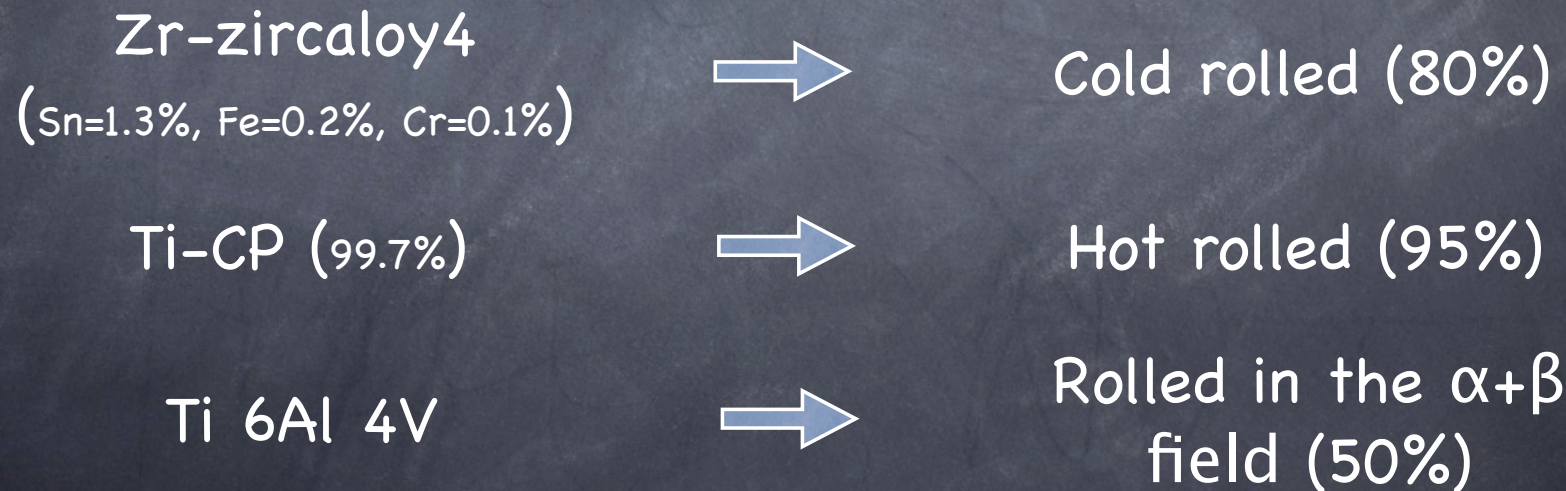
Material properties
anisotropy

Objectives of the work

To study the texture and α - β transition Zr and Ti alloys

To analyze the texture memory effect

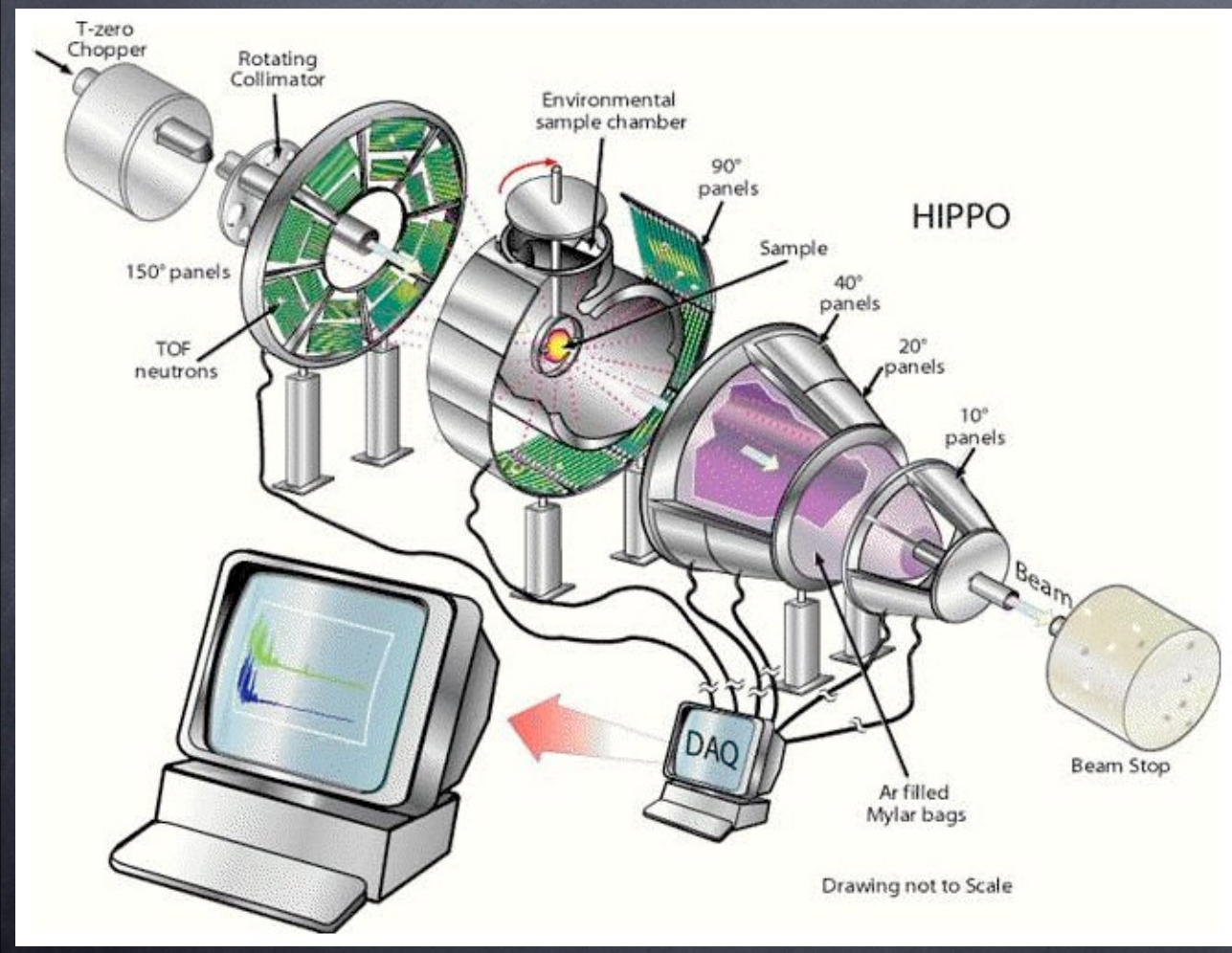
Three samples:



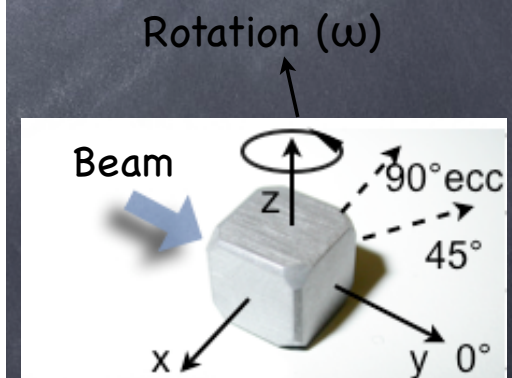
Measurements:

HIPPO(High Pressure Preferred Orientation)

LANSCE(Los Alamos Neutron Science Center)

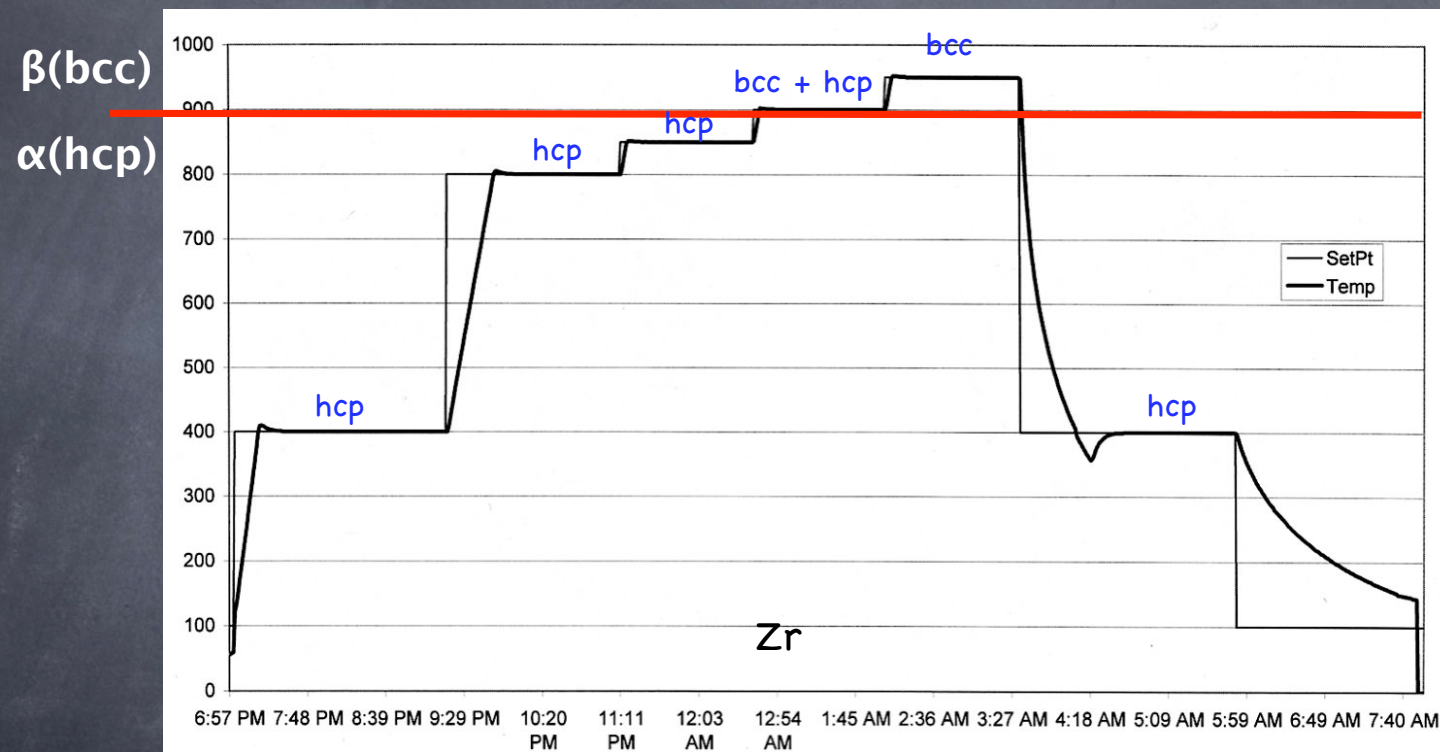


incident flight path 9 m
 2.4×10^7 neutrons $s^{-1} cm^{-2}$
 1360 3He tubes \rightarrow 50 panels
 cryogenic eq. (10-300 K)
 vacuum furnace (300-1400 K)
 anvil cell (20 GPa - 2000 K)
 gas cell (1 cm³, 10 kBar, 20 K)
 multi sample charger
 100 kN uniaxial load



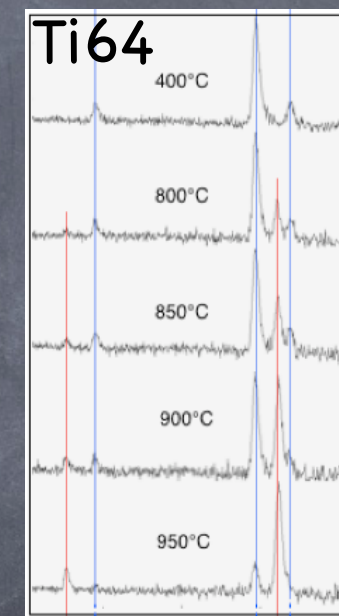
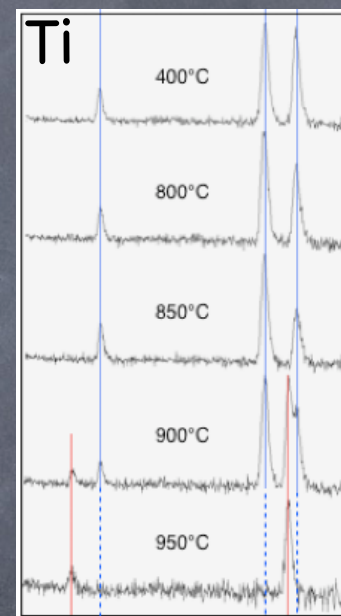
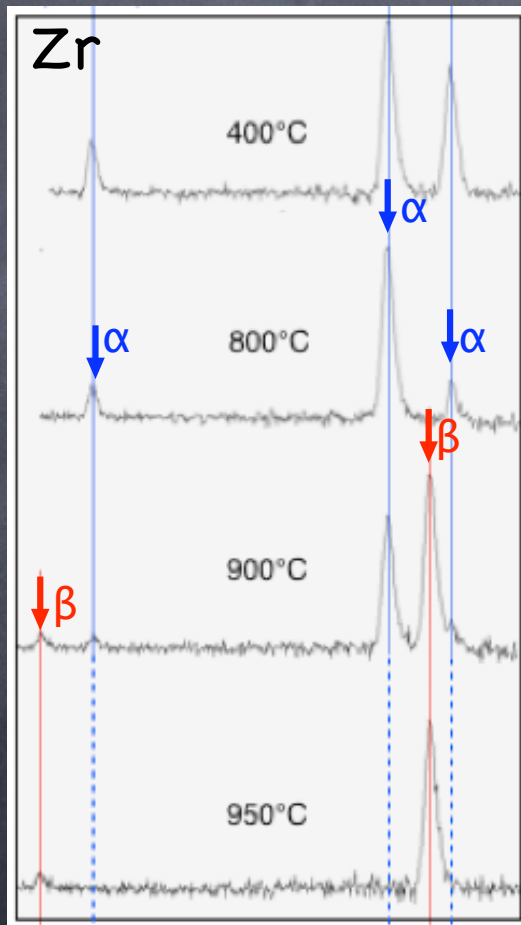
High temperature measurements for each sample

Zr: $T(\alpha-\beta) = 890^\circ\text{C}$

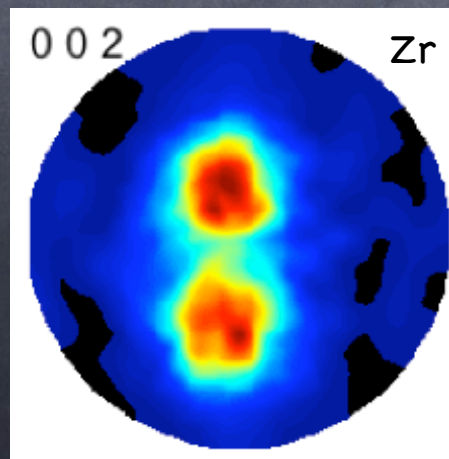
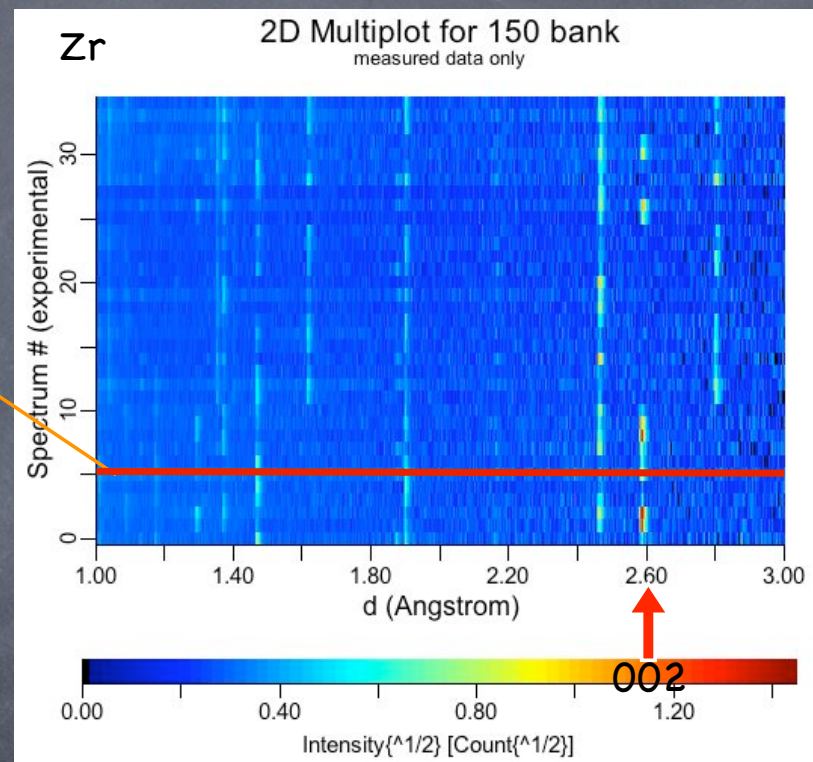
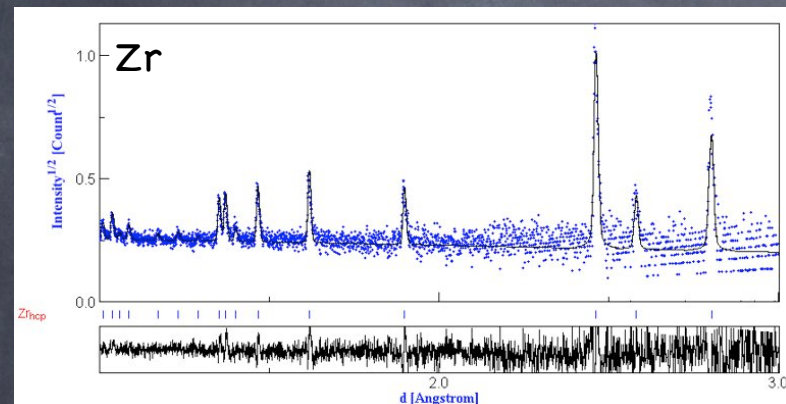


At each temperature a complete measurement for texture (rotating ω in step) was done

Zr, Ti, Ti64 the α - β - α transition



For each temperature step we have 120 TOF spectra for the Zr sample and 96 for Ti and Ti64

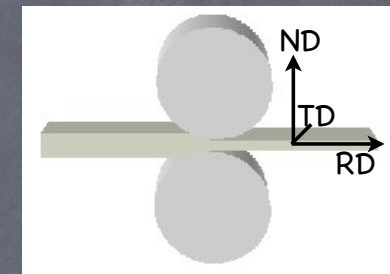
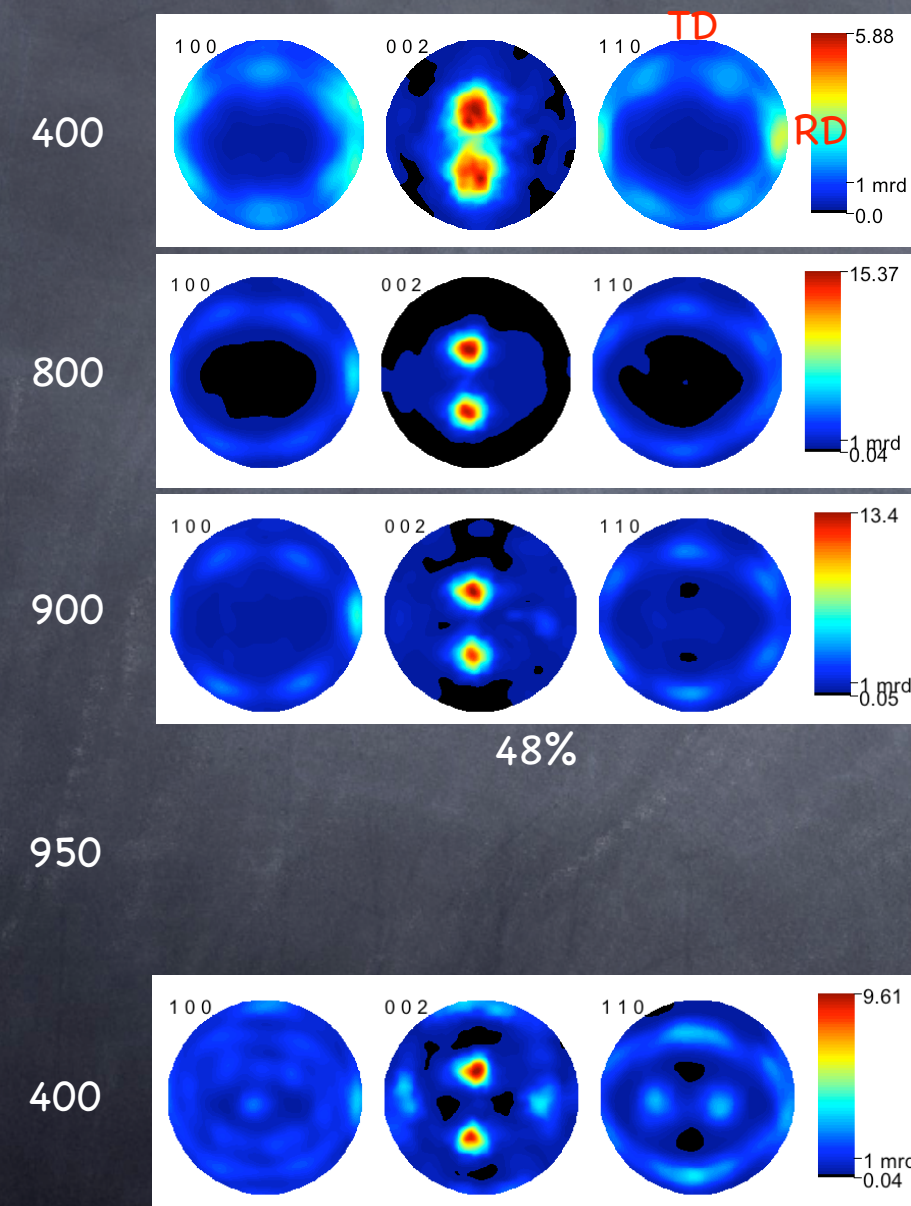


Reconstructed pole figures: zircaloy 4 (cold rolling, 80%)

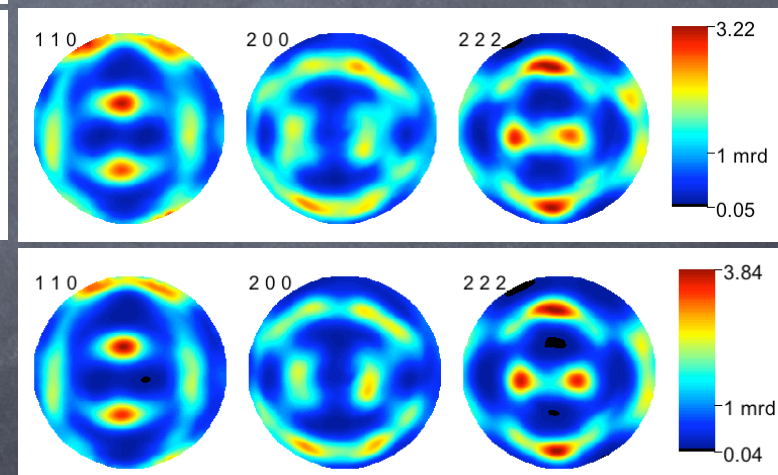
T (°C)

α phase (hcp)

β phase (bcc)



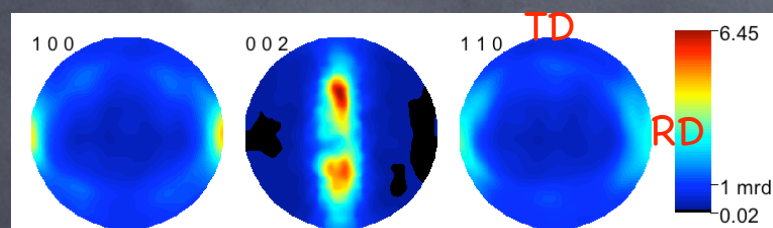
52%



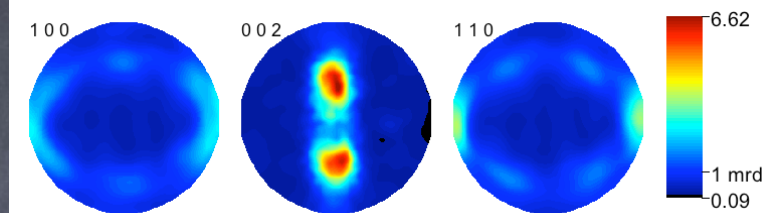
Reconstructed pole figures: Ti-cp (hot rolling, 95%)

T (°C)

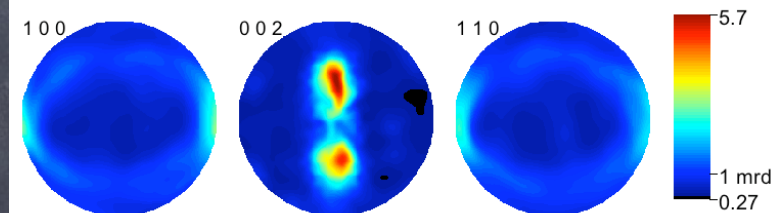
α phase (hcp)



800

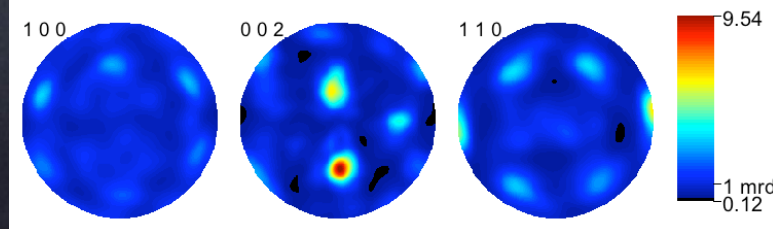


900

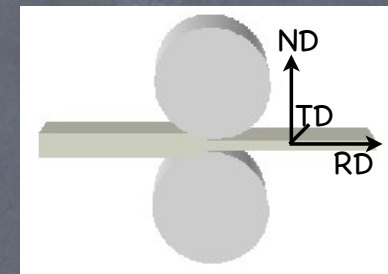


34%

950



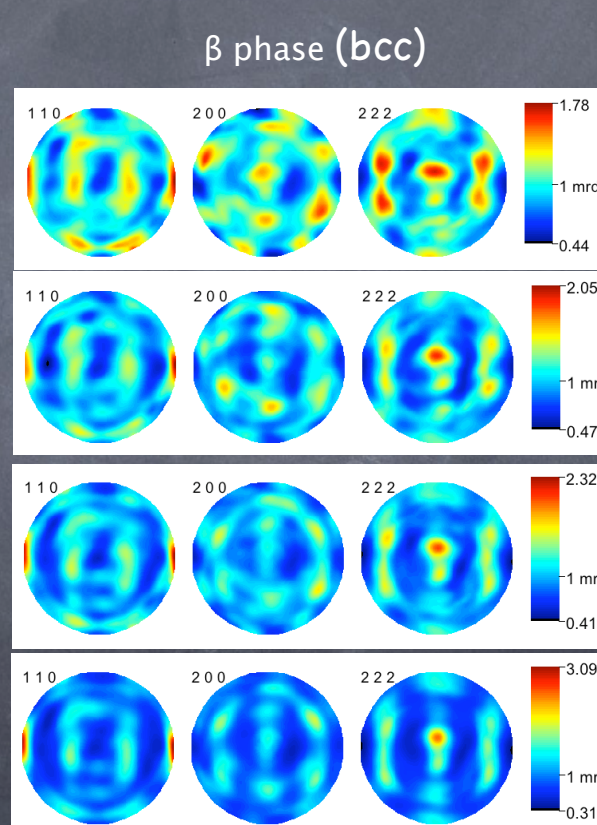
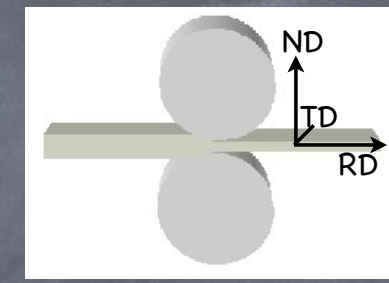
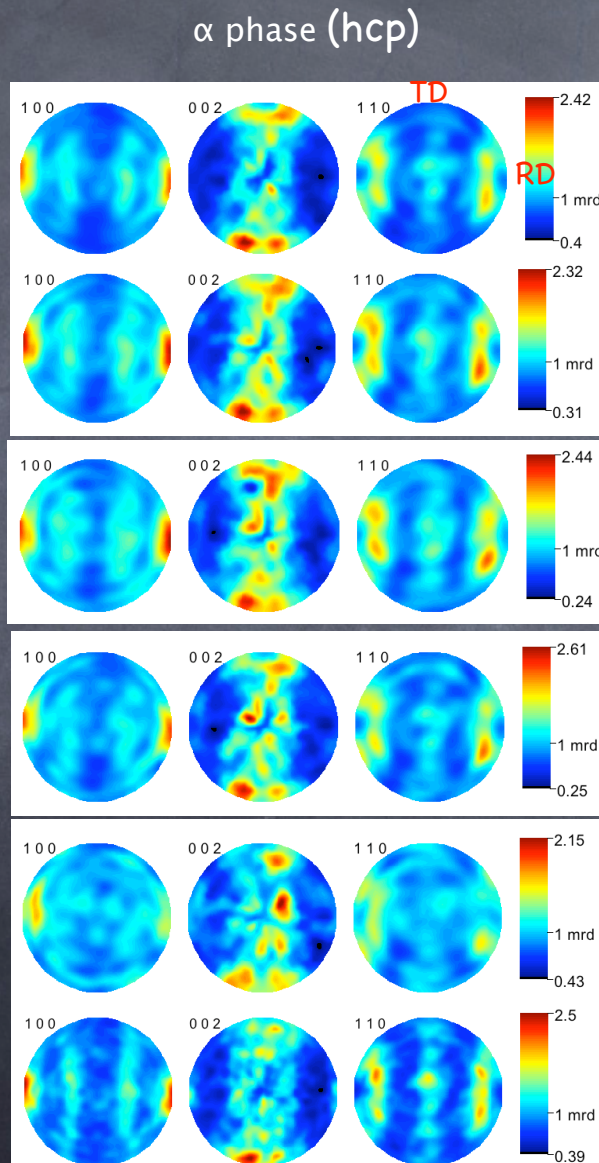
β phase (bcc)



66%

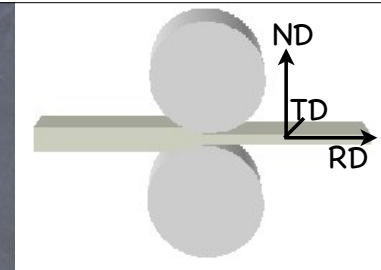
Reconstructed pole figures: Ti64 (rolled $\alpha+\beta$, 50%)

T (°C)	α phase (wt %)
400	95
800	80
850	74
900	57
950	22
400	92

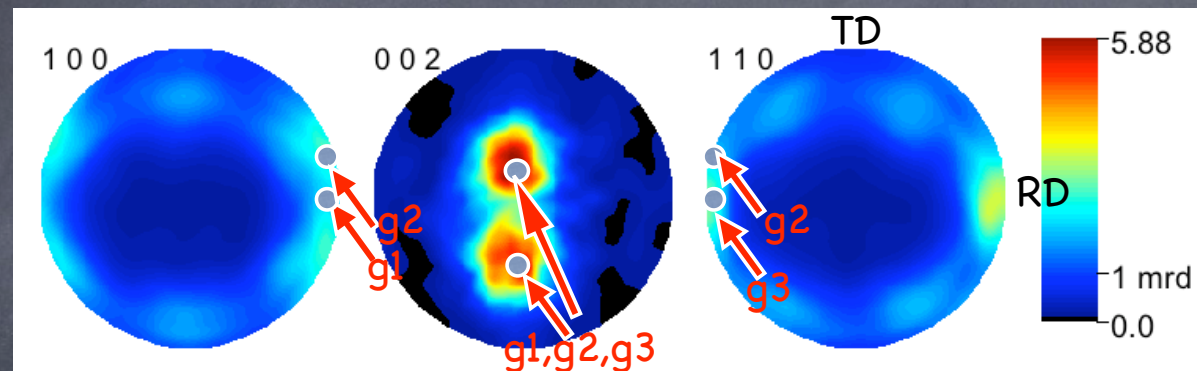


β phase (wt %)
5
20
26
43
78
8

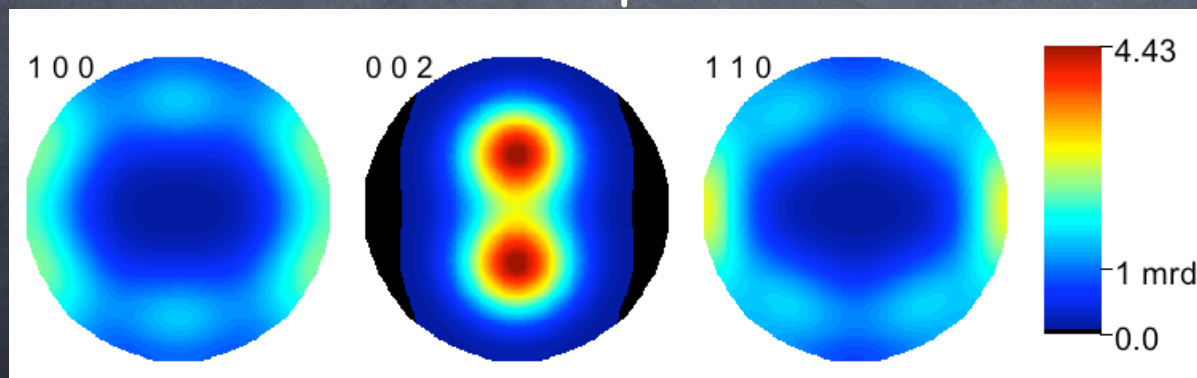
Texture analysis by components: Zr at 400°C



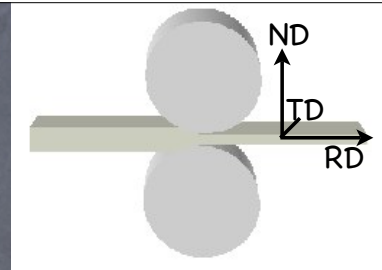
α -Zr: reconstructed PF from ODF



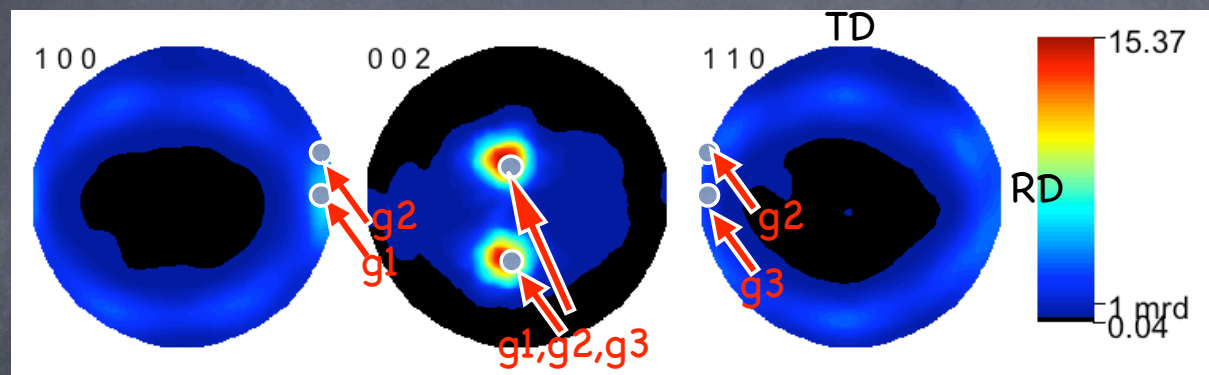
α -Zr: texture components simulation



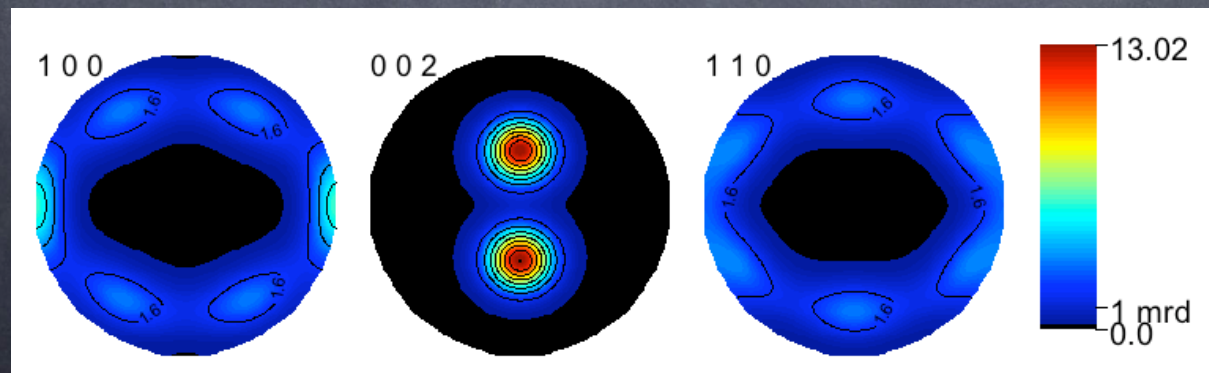
Texture analysis by components: Zr at 800°C



α -Zr: reconstructed PF from ODF



α -Zr: texture components simulation



α - β Zr transition: texture effect on Burgers relationships



(0002)hcp || (110)bcc
[-2110]hcp || [-11-1]bcc

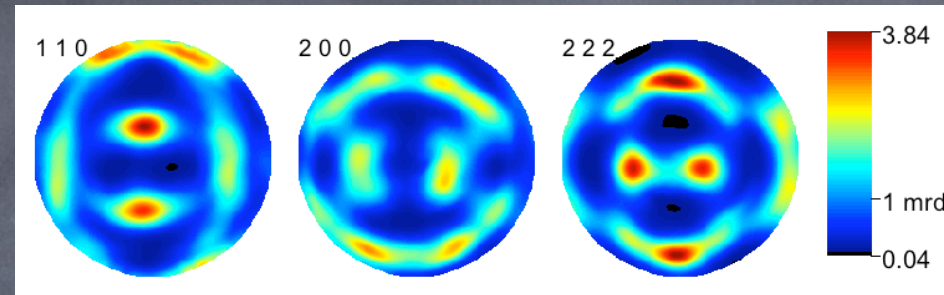


Six different variants in the α - β transition

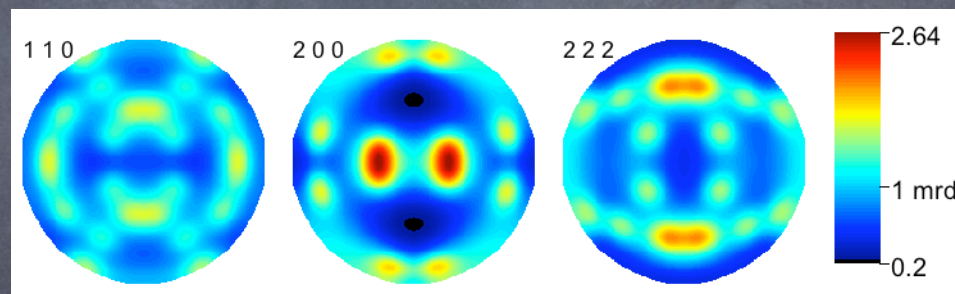
Variant index	plane (hcp) (bcc)	direction [hcp] [bcc]
1	(0001) (011)	[-2110] [-11-1]
2	(0001) (0-1-1)	[-2110] [-11-1]
3	(0001) (011)	[11-20] [-11-1]
4	(0001) (0-1-1)	[11-20] [-11-1]
5	(0001) (011)	[1-210] [-11-1]
6	(0001) (0-1-1)	[1-210] [-11-1]

Zr β (bcc) at 950°C

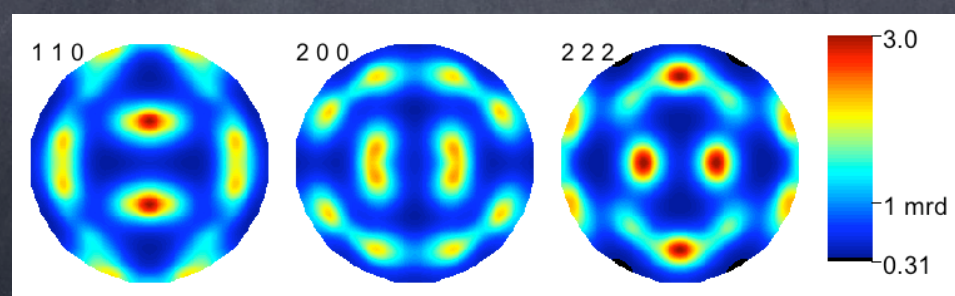
β Zr: PF reconstructed from measured ODF



All 6 Burgers variants applied to g1:



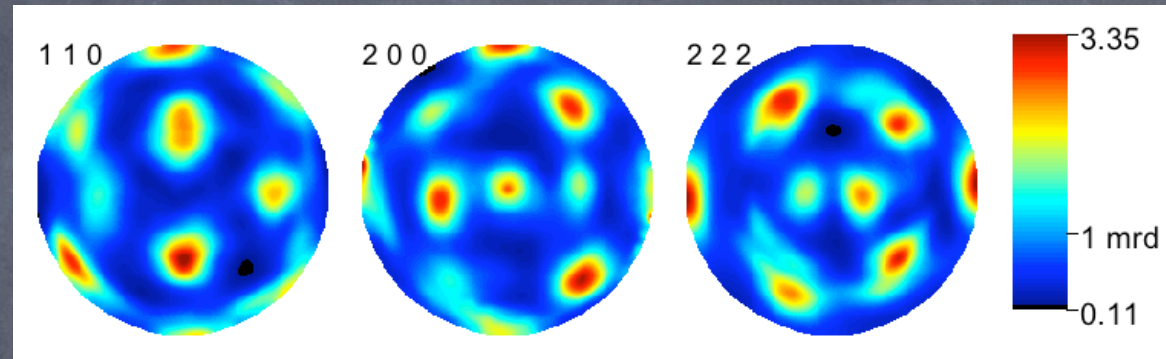
Using only variants 1, 2, 3, 6 on g1:



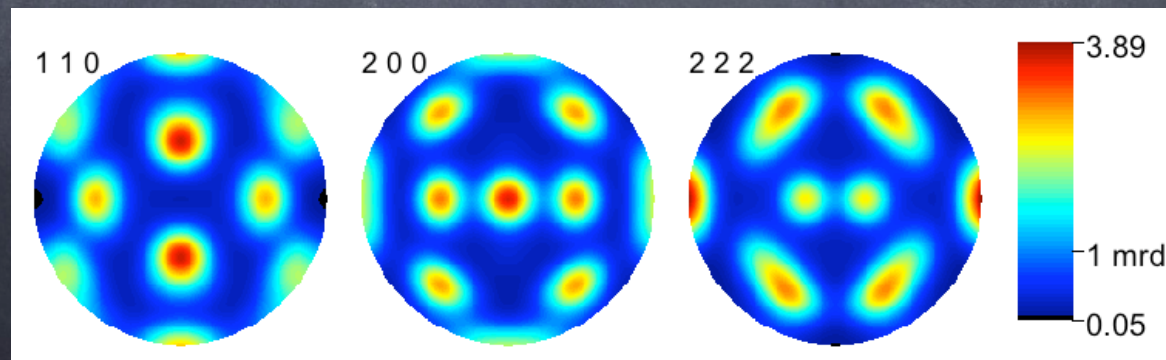
Ti-CP same methodology

All 6 variants are needed to simulate the texture-transition

950°C: measured PF



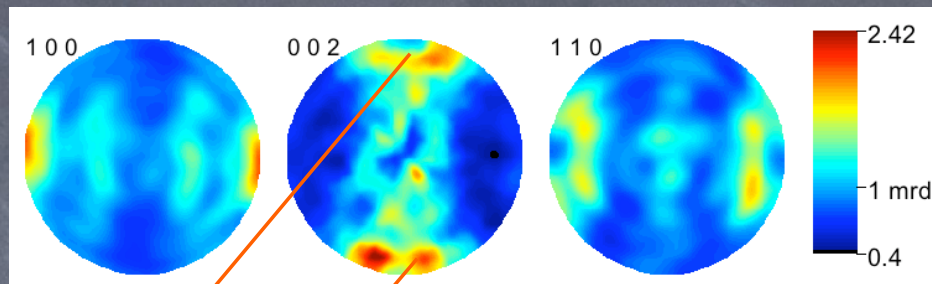
950°C: obtained from g1 and all 6 variants, no variants selection



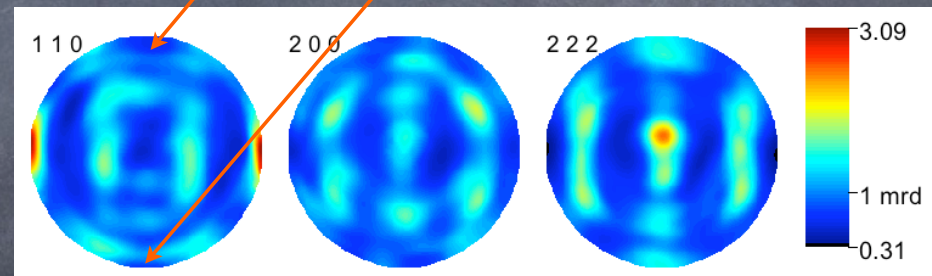
Ti64: no Burgers relationship/variant respected

~~(0002)hcp || (110)bcc
[-2110]hcp || [-11-1]bcc~~

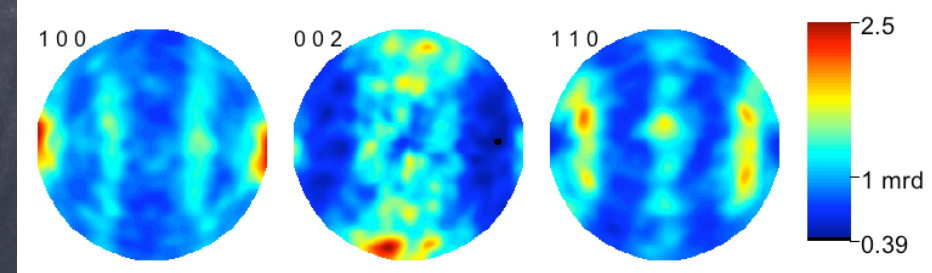
Ti64 α phase at 400°C



Ti64 β phase at 950°C

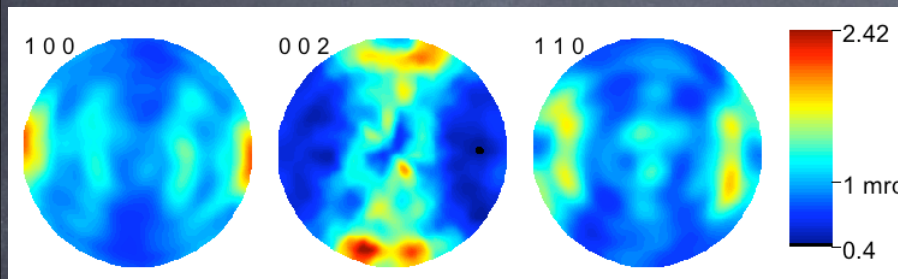


Ti64 α phase at 400°C

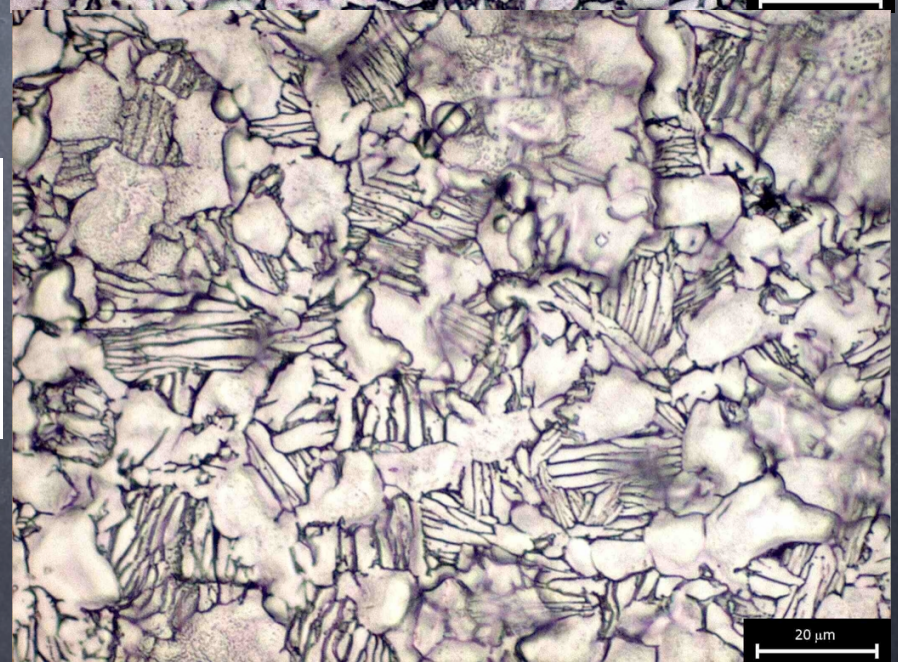
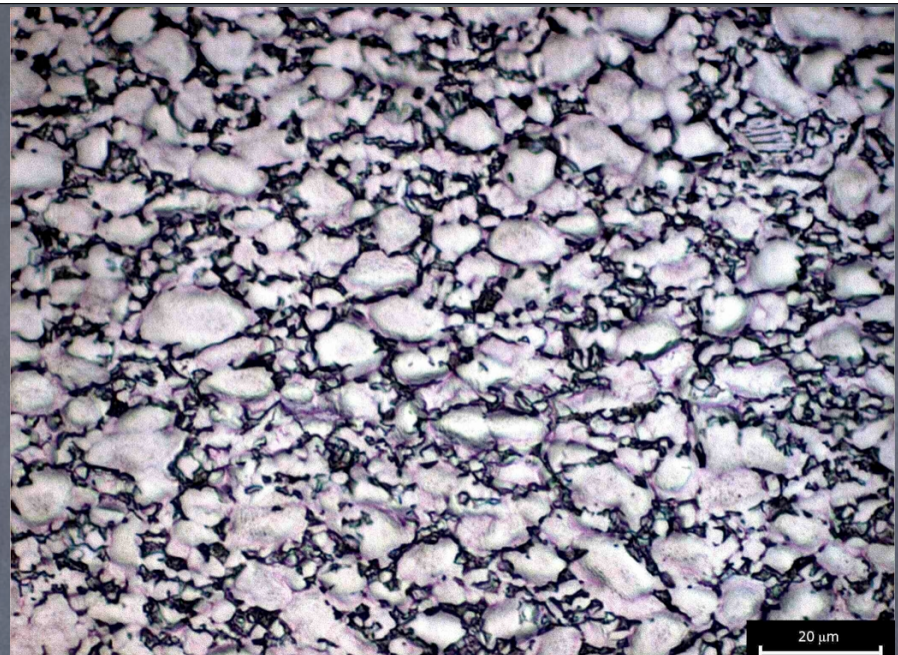
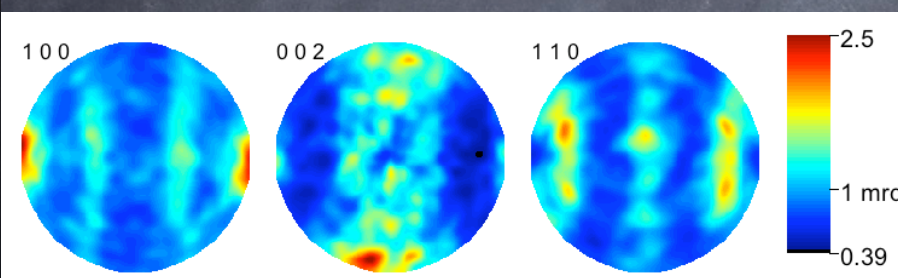


Ti64 and memory effect/ microstructure

Ti64 at 400°C before thermal treatment



Ti64 at 400°C after thermal treatment



Conclusioni

- Il metodo proposto mostra come sia possibile prevedere il comportamento a ricristallizzazione in relazione allo stato tessituro della lega di partenza
- Le transizioni polimorfe risentono della presenza di stato tessituro e in alcuni casi portano il materiale a delle selezioni
- Si sono osservati due tipi diversi di memoria di tessitura: uno come conseguenza di una selezione di orientazioni per Ti e Zr; l'altro legato alla presenza delle due fasi hcp e bcc (Ti64)
 - Questi aspetti si sono trovati per un unico ciclo termico: in futuro sarebbe interessante poter verificare se, con cicli termici ripetuti, tale effetto memoria si conserva
 - La metodologia seguita in questo lavoro potrebbe essere ripresa nello studio dell'effetto che la tessitura ha sulle leghe a memoria di forma

Future work

- ⌚ Busy days.....